Front. Earth Sci. 2022, 16(3): 601−622
https://doi.org/10.1007/s11707-021-0952-3

RESEARCH ARTICLE

Geochemical characteristics, genetic types, and controlling factors of natural gas in Jiyang Depression, Bohai Bay Basin (eastern China)

Tianchen GE[1], Xiangchun CHANG (✉)[1,2], Yuan ZHUANG[3], Xiaojun LI[4]

1 College of Earth Science and Engineering, Shandong University of Science and Technology, Qingdao 266590, China
2 Laboratory for Marine Mineral Resources, Qingdao National Laboratory for Marine Science and Technology, Qingdao 266071, China
3 School of Ocean and Earth Science, Tongji University, Shanghai 200092, China
4 Petroleum Exploration and Development Research Institute, Shengli Oilfield Company of SINOPEC, Dongying 257015, China

Abstract The Jiyang Depression is an important oil and gas production zone in the Bohai Bay Basin. Through a systematic investigation of the gas components and stable carbon isotopes, the genetic types of natural gas found in the Jiyang Depression were determined, that is, biogas, oil-associated gas, coal-derived gas, high-mature oil-related gas, and mantle-derived carbon dioxide (CO_2). From the results, natural gas in the Jiyang Depression can be divided into four groups. Group I, which is distributed in the northwest area, is the only typical oil-associated gas. Group II, distributed in the northeast area, is dominated by oil-associated gas, and involves biogas, coal-derived gas, and high-mature oil-related gas. Group III, distributed in the southeast area, has all genetic types of gas that are dominated by oil-associated gas and have mantle-derived CO_2. Group IV, distributed in the southwest area, is dominated by biogas and involves coal-derived gas and oil-associated gas. The differences in each group illustrate the lateral distribution of the natural gas types is characterized by the eastern and southern areas being more complex than the western and northern areas, the vertical distribution of gas reservoirs has no obvious evolutionary law. The main controlling factor analysis of the spatiotemporal changes of the gas reservoirs revealed that the synergy of geochemical characteristics, thermal evolution of the Shahejie Formation and Carboniferous-Permian source rocks, and sealing properties of various faults are jointly responsible for determining the gas reservoir spatiotemporal changes.

Keywords natural gas, genetic types, geochemical characteristics, distribution law, controlling factors, Jiyang Depression

Received May 3, 2021; accepted November 8, 2021

E-mail: xcchang@sina.com

1 Introduction

In recent years, the development concept "green mountains are gold mountains" has been widely accepted in China, and the importance of natural gas in the energy consumption structure has been increasingly improved. To date, significant achievements have been made in terms of the generation mechanism, origin discriminant, distribution of gas reservoirs, and migration and accumulation of natural gas (Song et al., 2014; Li et al., 2018, 2020; Wang and Li, 2020; Li et al., 2021a), which greatly facilitate the exploration of natural gas in China, such as in the Tarim Basin (Liu et al., 2018), Sichuan Basin (Wu et al., 2016), Junggar Basin (Hu et al., 2018; Chen et al., 2019; Li et al., 2019a).

The Jiyang Depression has been explored and developed for more than 50 years and still shows huge exploration potential (Vincent et al., 2011; Zhang et al., 2011; Cao et al., 2016). Although the Jiyang Depression possesses the second largest oilfield in China (Shengli Oilfield), its associated gas has been identified as small-scale and scattered. In the Jiyang Depression, the natural gas reservoirs are distributed in multiple sets of gas-bearing layers and occupy different tectonic positions (Zhang, 1991; Gan et al., 2005; Hu et al., 2021a). Previous studies have mainly focused on the genetic types, accumulation characteristics, enrichment model, and migration pathways of hydrocarbons in Minfeng Subsag (Li et al., 2005; Yang et al., 2014; Ping et al., 2017; Ci et al., 2020), Gubei-Bonan Subsags (Lin et al., 2007; Wang et al., 2007a; Guo et al., 2009; Jiang et al., 2009, 2010; Zhang et al., 2009), and Huagou-Pingfangwang-Pingnan Area (Hu et al., 2009; Meng et al., 2015), that is, most studies have focused on limited areas with certain gas types. Based on the large amount of analysis data from 30 gas fields of

different scales, this study attempted to improve the understanding of genetic type, distribution, and main controlling factors of natural gas discovered in the Jiyang Depression in order to facilitate further natural gas exploration.

2 Geological setting

Jiyang Depression, located in the southwest of the Bohai Bay Basin, is the biggest sub-unit of the Bohai Bay Basin (Fig. 1). It is the main petroleum-producing base for Shengli Oilfield. From 1960s to the present, the Jiyang Depression has proven crude oil reserves of about 50×10^8 t, and proven natural gas reserves of 2500×10^8 m^3, total production of oil is 10.7×10^8 t, and the natural gas is 460×10^8 m^3 (Li et al., 2003; Zhang, 2012; Song and Li, 2020). The Jiyang Depression is separated from Ludong Uplift in the east, and it is bounded by the Luxi Uplift in the south, and the Qingcheng-Linpanjia-Binxian highs in the west, the Chenjiazhuang high in the north. Many sub-depressions and highs were developed in the depression, covering from the southwest to the northeast (Chen et al., 2009). The sub-depression, i.e., Zhanhua, Dongying, Huimin, and Chezhen, respectively, can be further divided into different ternary structural units, which all showed good oil and gas generation and accumulation conditions (Fig. 1).

The tectonic evolution history of the Jiyang Depression comprised of three main stages. 1) Crystalline basement forming stage: the basement, Archean Taishan group, is a set of metamorphic rocks formed after Taishan Movement. 2) Platform sediments development stage (Palaeozoic-Mesozoic): in this stage, the depression experienced intensive uplifting, and marine and continental sediments alternately deposited. 3) Faulted depression-depression development stage: during this stage, the Jiyang Depression experienced Yanshanian movement and Himalayan movement successively, and developed a number of faults, accompanied by multiple episodic magmatic activity (Zhang, 2012; Zhang et al., 2020). The faults in the Jiyang Depression can be divided into three groups according to their occurrence, i.e., NE-, NW-, and near-E trending. Among them, NW-trending faults are mainly basin-controlling faults in the Late Jurassic–Early Cretaceous and Early Cenozoic. However, NE and near-E Faults are mainly active in the Cenozoic and Paleogene, especially in the Middle Eocene (Cai, 2008).

In terms of oil and gas forming conditions, five sets of high-quality gas source rocks were found in the Jiyang Depression, such as Carboniferous–Permian, Paleogene Kong 2 Member (Ek_2), Sha 4 Member (Es_4), Sha 3 Member (Es_3) and Sha 1 Member (Es_1). These source rocks possessed different organic matter type, burial depth, and thermal evolution, which make the types of gas generated complex and diverse. The natural gas reservoirs consisted of both hydrocarbon gas and non-hydrocarbon gas (mainly carbon dioxide). At present, 13 industrial gas-bearing layers have been discovered (Su et al., 2009; Li et al., 2015) covering Archaean, Paleozoic,

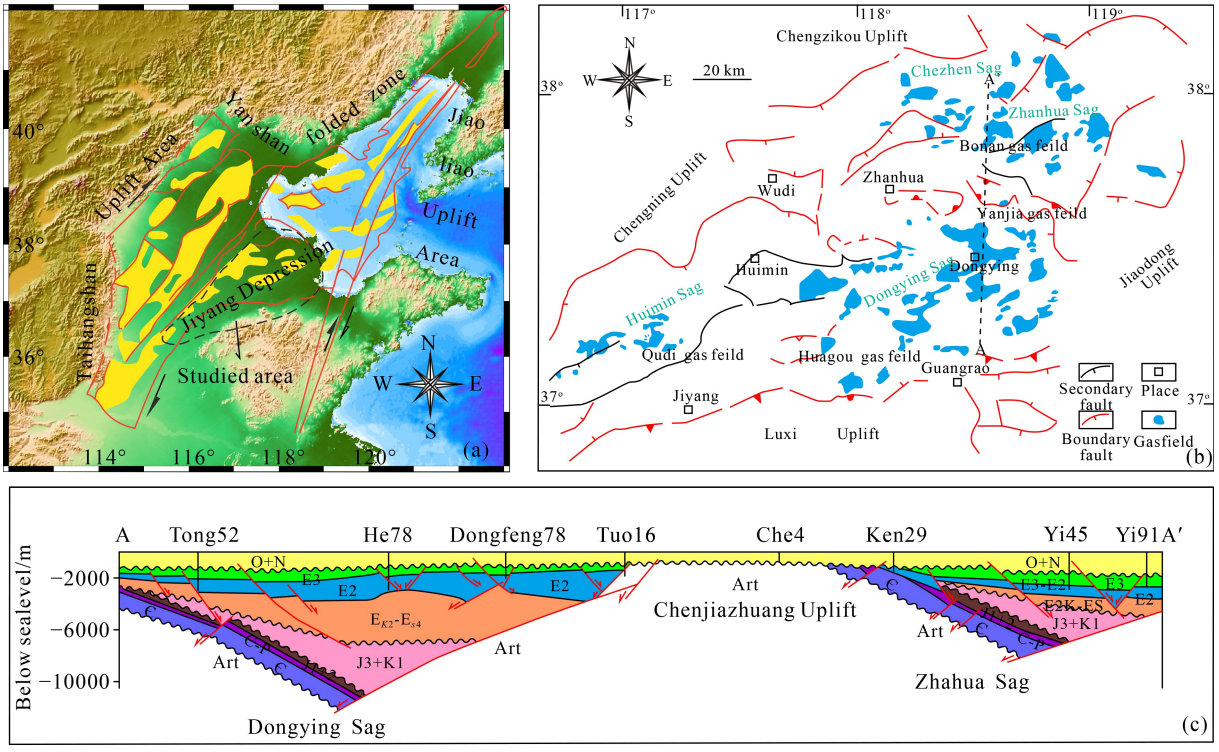

Fig. 1 (a) Location, (b) tectonic units and the distribution of gas fields and (c) stratigraphy section (A–A') in the Jiyang Depression.

Mesozoic, and Cenozoic intervals (Fig. 2). From the perspective of the genesis of natural gas, Jiyang Depression possessed oil-associated gas, coal-derived gas, and biogas, as well as inorganic mantle-derived carbon dioxide gas (Yang et al., 2019). The existence of various types of natural gas makes the Jiyang Depression become a promising exploration area.

3 Samples collection and methods

In this study, 139 natural gas samples from 29 gas fields in the Jiyang Depression were geochemically investigated. All samples were adopted from the database of the Shengli Oilfield Company and published literature (Song and Zhang, 2004; Zhu et al., 2005; Lin et al., 2007; Shen et al., 2007; Wang et al., 2007a; Wang et al., 2007b; Wang, 2008; Guo et al., 2009; Hu et al., 2009; Wang et al., 2009; Zhang et al., 2009; Li et al., 2010; Yang et al., 2014; Meng et al., 2015; Li W et al., 2015; Li Y et al., 2017). The natural gas samples involved in this study cover almost all the main gas production fields and formations in the Jiyang Depression. The characteristics of source rocks (including E*s* and Carboniferous–Permian) associated with natural gas samples are summarized in Table 1 (Zhou et al., 2006; Zhu et al., 2006; Wang et al., 2010; Zhang et al., 2011; Gao et al., 2020), mainly including total organic carbon (TOC), organic matter (OM), and vitrinite reflectance (R_o).

The natural gas compositions were measured using an Agilent 6890N gas chromatograph (GC). The stable carbon isotope compositions of the gases were measured using a Finnigan MAT-252 instrument. The TOC was measured using a LECOCS-230 analyzer after removing carbonate and washing with distilled water to remove residual hydrochloric acid (HCl). The R_o data were obtained using an oil immersion lens and a Leitz MVP-ST reflected-light microscope.

4 Results

4.1 Gas components characteristics

The results of 109 hydrocarbon gas samples from 29 gas fields are summarized in Table 2 and Table 3, and the results of 30 carbon dioxide (CO_2) gas samples are summarized in Table 4. As shown in Tables 1 and 2, for the hydrocarbon gases, the methane (CH_4) content ranges from 59.60% to 99.26%, with an average of 87.41%, and the content of heavy hydrocarbons (C_2^+) ranged from 0.11% to 38.79%, averaging 8.33%. The other gases include CO_2, accounting for 0.00 to 19.27%, with an average of 2.87%, followed by nitrogen gas (N_2), accounting for 0.00 to 24%, averaging 1.51%. The drying coefficients of those samples vary from 0.67 to 0.99 (average 0.91), suggesting a variable maturity of their source rocks. The samples' CH_4 content, C_2^+ content and drying coefficient with burial depth exhibited a good correlation (Fig. 3): whereas in the shallow and middle layers (< 3500 m), the CH_4 content and drying coefficient of the samples decreased with burial depth, and varied from typical dry gas to wet gas. It could be seen that as the depth increases, the CH_4 content and drying coefficient showed an increasing tendency in the deeper layers (3500–5500 m). Although the gas was still dominated by wet gas, it gradually changes to dry gas. As shown in Table 4, in CO_2 gas reservoirs, the content ranged from 57.41% to 98.59%, averaging 82.8%, showing typical inorganic genesis (Dai, 1993), while the other non-hydrocarbon gases were N_2, with contents ranging from 0.06% to 5.43%. The CH_4 content accounted for 0.44% to 42.59%, with an average of 12.21%.

4.2 Stable isotopes characteristics

The carbon isotopic values of all hydrocarbon gas sample exhibited a wide range: the carbon isotope of methane ($\delta^{13}C_1$) ranged from −63.2‰ to −32.7‰, while the $\delta^{13}C_2$ values fell between −38.3 ‰ and −16.8 ‰, the $\delta^{13}C_3$ ranged from −34.9 ‰ to −7.64 ‰, and the $\delta^{13}C_4$ varied between −32.1 ‰ and −14.9 ‰. The overall carbon isotopic composition of the alkanes follows the trend of $\delta^{13}C_1 < \delta^{13}C_2 < \delta^{13}C_3 < \delta^{13}C_4$, indicating a typical organic origin (Liu et al., 2018), and in some cases (i.e., the Gudao, Shanjiasi, Chenjiazhuang, Caoqiao, Kenxi, Bonan-Gubei, Zhuangxi and Gaoqing-Huagou Gas Fields) varied with the $\delta^{13}C_3 > \delta^{13}C_4$ (Fig. 4). By correlating the $\delta^{13}C_1$ value with the sample burial depth (Fig. 5), in the shallow strata (< 1500 m), the $\delta^{13}C_1$ value of most sample was between −40‰ and −55‰, and only a few samples were less than −55‰. Reaching the middle strata (1500−3500 m), the value is between −45‰−60‰, which is significantly reduced. Reaching the deep depth (3500−5500 m), the value increased obviously, ranging from −30‰ to −55‰, implying that the genetic types of gases vary with their burial depth.

For the CO_2 gas reservoirs, the $\delta^{13}C_1$ value was distributed from −54.39 ‰ to −42.51 ‰, and the carbon isotopes of the C_1 to C_4 alkane presented a positive-sequence distribution. The value of $\delta^{13}C_{CO_2}$ ranged from −9.8‰ to −3.35‰. It has been established that the isotope characteristics of the associated inert gases helium (He) and argon (Ar) are important indicators for the study of CO_2 gas reservoirs (Li et al., 2008; Hu et al., 2009; Ni et al., 2014; Liu et al., 2016a). For the samples of this study, the R/Ra value (where R is the $^3He/^4He$ value of the sample and Ra is the $^3He/^4He$ value of the atmosphere) of CO_2 was generally greater than 2, and the $^{40}Ar/^{36}Ar$ value was relatively high, ranging from 317 to 3000, and mostly higher than 1000.

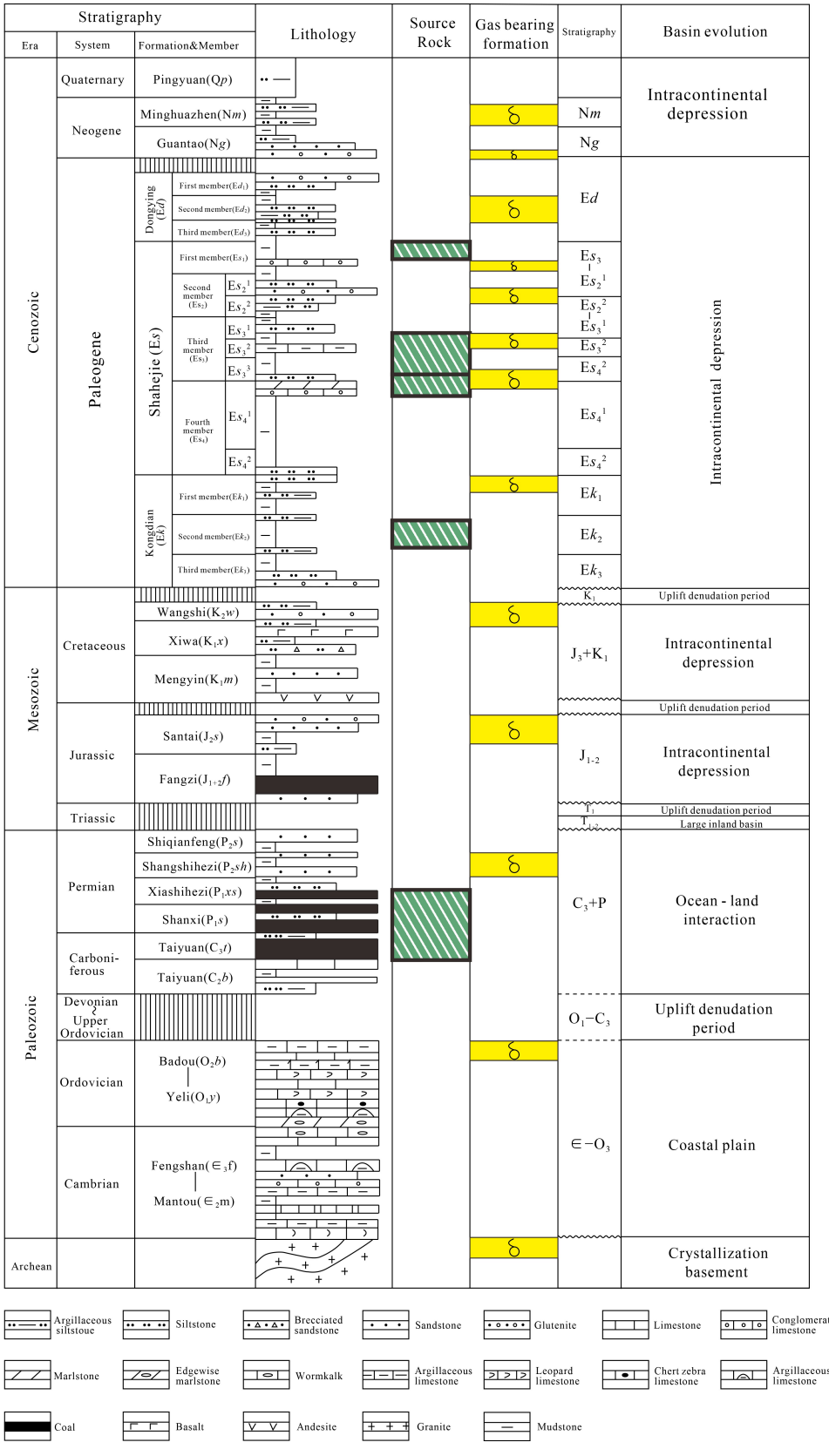

Fig. 2 Comprehensive histogram of the strata in the Jiyang Depression.

Table 1 Characteristics of source rocks in different areas of Jiyang Depression

Orientation	Source rock	TOC/%	Kerogen type	Buried depth/m	R_o/%	Thermal evolution stage	Associated gas reservoirs
Northwest	Es_1	1.0−8.0	I , II_1	1600−2800	<0.5	Immature stage	No gas reservoir formed
	Es_3	2.5−12.1	I , II_1	>3000	>0.5	Mature stage	Form crude oil associated gas reservoir
	Es_4	about 5.5	I , II_1			Mature stage	Form crude oil associated gas reservoir
	C–P	about 1.0	III	shallow	0.62−0.67	Mature stage	No gas reservoir formed
Northeast	Es_1	0.−7.0	I , II_1	<3000	0.43−0.60	Immature-mature stage	Form biogas reservoir
	Es_3	0.55−12.44	I , II_1	3200−3400	0.64−1.12	Mature stage	Form crude oil associated gas reservoir
	Es_4	0.77−15.18	I , II_1	>4000	0.8−1.56	Mature-high mature stage	Form high-mature oil-type gas reservoirs
	C–P	about 2.0	III	>3500	0.94−1.77	Mature-high mature stage	Form coal-type gas reservoirs
Southeast	Es_1	about 4.3	I	<1850	0.27−0.45	Immature-mature stage	Form biogas reservoir
	Es_3	0.7−3.9	I , II_1 (little II_2)	2000−4000	0.56−1.01	Mature stage	Form crude oil associated gas reservoir
	Es_4 Es_4^1	1.0−5.0	I , II_1 (little II_2)	2000−4000	0.58−1.30	Mature stage	Form crude oil associated gas reservoir
	Es_4^2	0.5−4.0	I , II_1,II_2	>4200	>1.2	High mature stage	Form high-mature oil-type gas reservoirs
	C–P	about 1.5	III	>3500	0.9−2.4	Mature-high mature stage	No gas reservoir formed
Southwest	Es_1	about 5.0	I	about 1750	<0.4	Immature-mature stage	Form biogas reservoir
	Es_3	about 3.0	I , II1	about 3000	>0.65	Mature stage	Form crude oil associated gas reservoir
	Es_4						
	C–P	about 2.0	III	>3000	0.85–2.20	Mature-high mature stage	Form coal-type gas reservoirs

Table 2 Gas component content and carbon isotope of alkanes in the northeast and northwest area of the Jiyang Depression

Group	Field	Well	Depth/m	Strata	Composition/%				δ^{13}C(VPDB‰)			
					N_2	CO_2	CH_4	C_{2+}	CH_4	C_2H_6	C_3H_8	C_4H_{10}
I	Dawangzhuang	DaG23	1738.3	O	/	2.04	90.18	7.23	−44.4	/	/	/
	Dongfenggang	Che57	4067	E	0.06	6.28	81.8	11.86	−44.2	/	/	/
II	Bonan	Yi11-381	2978–2988	E	0.61	14.95	72.56	11.8	−57.7	−38.3	−33.7	/
		Yi11-G25	2917–2927	E	0.74	8	75.17	15.8	−55.8	−36.4	−32.8	/
		Yi17	3397–3611	E	0.93	7.08	67.98	23.6	−59.4	−37.9	−32.0	/
		Yi171	3709–3735	E	0.75	7.52	74.61	16.7	−63.2	−38.1	−29.7	/
		BoS4	3898–3924	E	1.53	1.4	83.38	14.59	−52.7	−30.8	−28.2	−28.1
		Yi11	2892–2905	E	1.15	2.87	76.42	18.21	−53.7	−35.3	−31.1	−29.6
		XinYi12	2454.9	E	/	4.3	74.78	20.5	−52.3	−33	−31.2	−29.8
		Yi37	3220.3	E	/	9.55	66.2	22.45	−45.6	−31.7	−32.9	−28.3
		Yi52	2943–2962	E	/	6.25	71.42	20.32	−54.2	−36	−33.0	−30.6
		Yi99	3168–3206	E	/	10.89	56.9	23.96	−48.4	−33.1	−31.3	−29.8
		Yi170	3806–3829	E	0.14	2.72	84.44	12.4	−52.6	−31.2	−27.3	−27.2
		Luo36-1	2344–2369	E	/	/	/	/	−53.3	−37.5	−34.9	−31.7
		BoS6-5	4391–5118	O	0.98	6.66	71.83	19.67	−41.5	−28.2	−25.2	−25.0
		BoS6	4165–4434	O	0.51	4.77	74.98	19.27	−40.8	−27.6	−24.5	−24.8
		Bo601	5007–5009	O	1.22	5.05	76.2	17.27	−43.8	−28.7	−25.8	−26.1
		BoS3	4450–4472	E	1.28	8.03	77.06	16.03	−39.1	−26.7	−23.4	−23.9
		Yi115	5144–5163	E	0.05	19.27	80.18	0.51	−35.9	−24.9	−21.8	/
		Yi115	5144–5163	E	/	7.38	88.29	4.33	−37.7	−25	−24.8	/
		BoG4	4375–4460	O	0.44	7.39	81.96	10.18	−38.2	−24.9	−22.5	−23.6
		Yi121	4426–4438	E	/	7.09	91.36	1.46	−38	−22	−19.3	−20.6
		BoG403	3806.55–3966	O	1.5	6.65	78.66	12.73	−37.1	−23.4	−22.4	−23.4
	Chengdao	ChengBS19	1308.2	N	0.37	0.2	98.03	1.2	−53.9	−36.2	−34.9	−32.1
		ChengB12	2144.5	E	0.62	0.63	60.63	38.79	−38.0	−28.3	−27.8	−27.1
		ChengB242	2936.6	Pz	0.29	2.26	70.97	26.37	−45.7	−31.2	−28.9	−28.1
	Laohekou	ChengB39	4173–4320	Pz	2.04	7.48	75.02	15.47	−1.3	−7.6	−5.9	−25.7
	GuBei	Bo93	3230–3249.4	C–P	/	2.29	88.99	7.97	−38.1	−22.7	−21.3	−21.8
		Bo93	3120–3136	C–P	0.55	1.47	92.1	5.88	−37.1	−19.1	−17.1	−18.8
		Bo930	3617.1–3639.2	C–P	0.65	7.7	86 .15	5.50	−35.50	−16.8	−16.1	−15.4
		Yi132	3374–3387	C–P	0.98	1.87	82.1	14.21	−36.97	−25.4	−25.0	−25.5
		Yi155	4528.8–4574	C–P	0.86	6.64	87.64	4.85	−32.2	−22	−21.5	−21
		GuBG1	4020.65–4139.5	C–P	0.39	5.3	86 .96	7 .31	−35.90	−23.1	−21.2	−21.2
		GuBG1	4120.6–4139	C–P	0.74	6.66	82.52	10.09	−35.8	−22.9	−21.5	−20.8
		GuBG2	3517.7–3534.2	C–P	1.31	0.09	95 .02	3 .58	−36.30	−22.5	−21.8	−22.0
		GuBG2	3517.7−3534.2	C–P	0.96	3.65	75.87	19.48	−41	−25.8	−23.6	−23.6
	Zhuangxi	Zhuang202	2644.5	E	/	1.13	86.22	7.49	−51.6	−34.9	−31.7	−29.4
		Zhuang50	3228.2	E	/	1.73	89.44	7.47	−49.7	−33.5	−30.1	−28.2
		Zhuang74	3634.5	E	/	4.81	68.44	23.49	−47.6	−33.3	−28.9	−27.5
		ZhuangG21	3929.1	O	/	3.13	67.15	25.73	−42.4	−27.9	−27.7	−26.4
		ZhuangG25	4277.6	∈–Anz	/	1.36	71.34	25.48	−43.2	−29.7	−26.3	−27.7
		ZhuangG17	4886.2	∈	0.58	3.09	85.99	10.25	−45.8	−31.9	−29.2	−28.5
		ZhuangG14	4318.5	O	/	9.24	76.77	13.21	−46.1	−32	−29.6	/
		ZhuangG13	4367.5	O	/	1.87	69.54	27.75	−42.2	−29.5	−28.1	−27.2
		ZhuangG23	3897–3988.5	O	1.14	1.53	86.38	10.65	−38.3	−27.6	−23.3	−26.2
	Chengdong	ChengK1	2588	P	0.18	0.71	73.92	25.53	−51.5	−34.1	−31.7	−29.8
	Yanjia	Yan22	1573	E	0.39	3.45	70.77	25.39	−47.4	−33.5	−29.2	−27.7
	Yonganzhen	Yong12-21	/	E	1.28	1.109	98.55	1.28	−47.6	−39.9	−31.7	−28.5
	Chenjiazhuang	Chen7-2	1300.1	N	/	/	98.11	1.1	−47.5	−33.7	/	/
		ChenQ11	935–942	N	4.706	0.122	95.02	0.152	−52.9	−33.1	−20.1	−18.5
		ChenQ8	945–948	N	10.49	0.752	88.44	0.315	−53.9	−25.7	−27.1	−29
	Gudao	GuD22-3	1214.8–1219.6	N	0.26	0.13	97.17	2.41	−43.7	−30.6	−23.3	−22.4
		GuD29-416	1246–1270.4	N	1.52	1.83	94.99	1.6	−45.9	−29.1	−23	−21.1
		GuD3-015	1203.7–1207.4	N	0.33	0.54	95.19	3.92	−45.4	−30.7	−26.1	−23.3
		GuD31-15	1196.2–1238.2	N	0.83	0.51	93.51	5.01	−45.6	−30.3	−25.6	−23.6

(*Continued*)

Group	Field	Well	Depth/m	Strata	Composition/%				δ^{13}C(VPDB‰)			
					N_2	CO_2	CH_4	C_{2+}	CH_4	C_2H_6	C_3H_8	C_4H_{10}
		GuD2-2	1191–1204	N	/	1.27	90.42	8.1	−41.9	−31.1	−27.8	−25.5
		GuD2-5	1175.2–1204.2	N	12.41	1.63	73.28	12.42	−41.8	−31.4	−27.7	−25.2
		GuD22-N3	1261.6–1294	N	0.28	1.15	93.12	5.42	−42.3	−31.3	−26	−23.9
		GuD13-N11	1252.8–1263.6	N	0.45	0.71	93.57	5.2	−41.9	−32.1	−27.7	−24.8
		GuD13-P513	1380.5–1562	N	0.5	0.56	88.25	10.59	−42.2	−31.9	−27.5	−25
		GuQZ6-13	1094.9	N	/	/	97.86	1.38	−42	−23.5	−15.2	/
		GudaoQ27-3	1065.2	N	/	/	97.24	2.69	−41.4	−25.9	−14.9	−14.9
	Kenxi	Ken126-X1	1646	N	1.38	1.66	91.9	4.82	−39	−33.6	−29.3	−26.3
		Ken71-75	1435	N	0.44	0.5	95.9	3.06	−42.3	−33	−25.7	−24.9
		KenX125	1638	N	0.48	0.94	91.74	6.77	−44.6	−31.7	−7.64	−15.6
		Ken23-5	1099	N	1.07	0.12	98	0.81	−43.4	−32.6	−29.1	−26.2
		Ken23-QX52	1154	N	1.6	/	97.99	0.41	−50	−19.5	/	/
		Ken71-75	1435	N	0.44	0.5	95.9	3.06	−42.3	−33	−25.7	−24.9
	GuDong	GuDong9	2506.4	E	24	2.52	60.05	20.99	−48.7	−27.4	−27.3	−25.6
		GuDong10	1321	N	/	/	95.21	2.49	−40.8	−29.1	−16.2	−21.5
		GuDong20-20	1416.4	N	/	/	96.43	1.55	−40.7	−29.6	−17.3	−20.1
		GuDong22-375	1311.95	N	/	/	95.01	4.1	−41.4	−26	−14.8	−21.6
		GuDong31-12	1367.85	N	/	1.02	95.22	2.58	−41.9	−29	−14	−16.8
		GuDong33	1539	N	/	/	96.89	3.15	−39	−34.8	−23.2	−24.9
		GuDong36-335	1310.25	N	/	0.37	95.86	3.95	−44.5	−29.6	−18.6	−21.4
		GuDong7	1306.15	N	1.75	0.16	96.98	1.11	−42.8	−29.2	−19	−23.2
		GuDongZ3-15	1389.5	N	0.11	0.59	95.04	4.18	−40.5	−37.7	−19.1	−21.8
		GuX1-11	1006.75	N	/	/	98.11	1.06	−41.3	−22.6	−13.4	/

5 Discussion

To facilitate the study, we divided gas samples into four groups: **1) Group I:** comprising the samples from Dongfenggang and Dawangzhuang Gas Fields, located in the northwest part of the depression; **2) Group II:** comprising the samples from Chengdao, Laohekou, Zhuangxi, Chengdong, Bonan-Gubei, Gudao, Gudong, Kenxi, Chenjiazhuang, Yanjia, and Yonganzhen Gas Fields, located in northeast part of the depression; **3) Group III:** comprising the samples from Minfeng, Guangli, Lijin, Xianhe, Shengtuo, Shanjiasi, Liangjialou, Pingfangwang, Pingnan, Gaoqing, and Huagou Gas Fields, located in southeast part of the depression; **4) Group IV:** comprising the samples from Qudi, Yuhuangmiao, Balipo, and Yangxin gas fields, located in the southwest part of the depression.

5.1 Genetic types of natural gas

Gas components and stable carbon isotope characteristics are often widely used as measurements for the classification of natural gas genetic groups, gas–gas and gas–source rock correlation, evaluation of maturity, and determination of gas migration direction and distance (Dai, 1990, 1992; Clayton, 1991; Dai et al., 2005, 2012, 2014, 2016; Ni et al., 2013; Shi et al., 2019, 2020a, 2020b; Hu et al., 2021b).

5.1.1 Genetic types of samples in north depression

For Group I, the CH_4 content was greater than 80%, and the corresponding drying coefficients were also higher than 0.85, while the $\delta^{13}C_1$ values were lower than −40‰ (Table 2). These characteristics indicate that Group I gas is oil-associated gas. For Group II, as listed in Table. 1, the characteristics vary greatly. The minimum CH_4 content reached 56.9%, the minimum value of $\delta^{13}C_1$ reached −63.2‰, and the maximum value of $\delta^{13}C_2$ was −16.8‰. Some samples from Group II showed carbon isotope reversion, that is, $\delta^{13}C_3 > \delta^{13}C_4$ (Fig. 4). It is thought that the reversed alkane carbon isotope trend can result from a variety of processes related to thermal effects, or mixing of the oil-associated gas and coal-derived gas, or the effects of secondary alteration (Cai et al., 2001; Dai et al., 2004; Hao et al., 2008; Liu et al., 2018). The $\delta^{13}C_3$ value of Group II, whose gas samples originate from the Gudao, Shanjiasi, Chenjiazhuang, Caoqiao, Kenxi and Gaoqing-Huagou Gas Fields, was nearly 5‰ higher than the value of $\delta^{13}C_4$; meanwhile, the propane content of Group II was lowest, and the drying coefficient was higher than 0.90, indicating that these gases are influenced by biological processes. However, for the Group II samples from the Bonan-Gubei and Zhuangxi Gas Fields, although the reversal phenomenon was similar to that in the above areas, the burial depth of these gases was sufficiently deep so as to exclude the

Table 3 Gas component content and carbon isotope of alkanes in the Southeast and Southwest area of the Jiyang Depression

Group	Field	Well	Depth/m	Strata	Composition/%				δ^{13}C(VPDB‰)			
					N_2	CO_2	CH_4	C_{2+}	CH_4	C_2H_6	C_3H_8	C_4H_{10}
III	Guangli	Lai10	2665.1	E	/	0.46	81.35	15.39	−50.6	/	/	/
	Xianhe	Niu23	3289.8	E	/	4.05	73.2	20.13	−52.1	/	/	/
		Wang53	3389	E	/	4.99	67.63	23.94	−50.4	/	/	/
	Liangjialou	Liang60	2844.8	E	/	3.61	73.12	20.23	−52.3			
		Liang35	3119.9	E	/	1.28	89.84	5.93	−50.8	/	/	/
	Panhe	Lin2-4	1398.8–1426	N	2.49	0.16	96.62	0.719	−47.6	−29.3	−16.2	−20.8
		Lin2-6	1582.8	N	0.59	0.17	96.6	2.728	−44.5	−32.5	−26.7	−27.7
	Shengtuo	Tuo765	4354.1–4386	E	0	0.15	87.82	12.03	−43.9	−28.6	−24.9	−26.6
	Lijin	XinLiS1	4271.2–4374	E	/	/	86.4	9.84	−41.8	−23.5	−24.4	
		LiS101	4371.3–4464.8	E	/	/	88.1	8.67	−40.9	−23.9	−20.8	/
	Minfeng	FengS1	4316.6–4343	E	1.6	5.74	81.58	16.3	−50.4	−30.8	−26.8	−25.8
		FengS1	4400	E	0.53	16.28	71.39	11.64	−48	−34	−27.3	−25.6
		Feng8	3935–4226	E	0.53	0.84	78.3	20.29	−49	−32.4	−28	/
		FengS3	4740–4847	E	0.08	3.16	92.16	4.68	−44.7	−30.1	−23.4	−23.2
	Shanjiasi	Shan66	1076–1100	Anz	0	1.61	95.85	0.41	−46.8	−29.9	−18.9	−24.1
		Shan2-1	1152.4	E	1.57	1.38	95.91	1.14	−48.7	−30.7	−24.3	−26.4
		Shan2-9	1167.5	E	1.43	1.91	95.34	1.22	−48.9	−30.3	−22.3	−25.9
	Gaoqing	Gao41-5	1034.9	Mz	/	0.82	97.38	1.65	−41.8	−25.1	−8.52	−22.1
		Gao42	948.8	E	1.03	1.23	97	0.8	−43	−32	−16.5	−23.1
	Caoqiao	Cao104	1258–1265.6	E	1.23	0.42	97.87	0.4	−46.4	−35.7	−23	−22.1
		CaoQ20-X22	1247	N	1.93	0.15	97.64	0.27	−42.8	−21.8	/	/
		CaoQ20-11	1170	N	1.6	/	98.06	0.32	−46.2	−24.6	/	/
	Huagou	Hua4	1276.1–1282.0	E	7.9	0.08	88.83	1.85	−55.2	−30.9	−22.4	
		Hua6	818.0–819.6	N	/	0.02	99.26	0.44	−44.3	−25.2	−20.3	
		Hua16	828.1–831.0	N	0	0.71	98.99	0.31	−46.6	−30.4	−22.6	−26.1
		Hua6-2	790.0–830.0	N	1.11	1.93	96.5	0.43	−44.4	−24.9	−20.1	−24.9
IV	Yangxin	Yang101	1276.1–1282.0	E	1.04	0.39	98.4	0.17	−60.6	/	/	
		Yang16	1276.1–1282.0	E	2.17	2.98	94.66	0.19	−56.5	/	/	
		Yang21	1276.1–1282.0	E	1.69	0.1	97.16	0.08	−60.9	/	/	
	Qudi	QuG1	1514–1520	E	11.9	0.93	77.25	9.53	−32.6	−23.9	−20.3	−20.2
	Yuhuangmiao	Xia8	1457.7–1464	E	/	/	98	0.9	−47	−32.5	−22	−22.8

effects of biodegradation, hence the real reason for partial reversal is related to the several sets of source rocks being comprised of matured E*s* (Types I and II), Mesozoic coal-measure source rocks (Type III) with different OM types, which produced mixed gas.

Typically, $\delta^{13}C_2$ values of −28‰ and $\delta^{13}C_3$ values are generally considered as the criteria for identifying oil-associated gas from coal-derived gas (Liu et al., 2019). Figure 6 displays the correlation between $\delta^{13}C_2$ and $\delta^{13}C_3$, Family II gas from Zhuangxi, Chengdao, Yanjia, Yonganzhen, Chenjiazhuang, and part of the Bonan Gas Fields (Wells BoS4, Yi11, XinYi12, Yi37, Yi52, Yi99, Yi170, Luo36-1, and BoS6-5) have values of $\delta^{13}C_2$ less than −28 ‰ and a $\delta^{13}C_3$ value less than −25 ‰, which demonstrates a typical pattern of thermogenic oil-associated gas. Furthermore, gases from the Gubei Gas Field, part of Bonan (Well Yi115, Yi121, BoG4, and BoG403) Gas Field, and well Gux1-11, reveal characteristics contrary to the above samples, in that they show typical patterns of thermogenic coal-derived gas.

These conclusions are further supported by the cross-plots of $\delta^{13}C_1$, $\delta^{13}C_2$, and $\delta^{13}C_3$ (Fig. 7) of natural gas and the C_1/C_{2+3} and $\delta^{13}C_1$ identification diagram of natural gas (Fig. 8), which were proposed by Dai (1990). The above samples confirm the carbon isotope threshold of oil-associated gas fall in zones II and IV in Fig. 7, and

Table 4 Molecular and isotope compositions of carbon dioxide gas reservoirs in the Jiyang Depression

Group	Field	Well	Depth/m	Strata	Composition/%				$\delta^{13}C$(VPDB‰)					R/Ra	$^{40}Ar/^{36}Ar$
					N_2	CO_2	CH_4	C_{2+}	CH_4	C_2H_6	C_3H_8	C_4H_{10}	CO_2		
III	Pingfangwang	Bin4-6-6	1469.7–1481	E	0.33	72.5	23.52	3.53	−51.7	−33.2	−29.8	−28.5	−4.57	2.76	1791
		Bin14-3-1	1453–1455	E	0.85	72.67	22.71	3.77	−52.7	/	/	/	−5.08	2.76	600
		PingQ4	1459.4–1474.5	E	0.46	75.33	20.89	3.27	−51.7	−33	−30	−29	−4.52	2.75	1758
		PingQ9-3	1462.6–1489.2	E	0.25	73.87	22.46	3.36	−51.6	/	/	/	−4.47	2.76	317
		PingQ12	1470.5–1498	E	0.63	74.2	21.63	3.39	−51.9	/	/	/	-4.36	2.75	1051
		PingQ12-61	1452.4–1487.6	E	0.38	79.17	17.13	3.19	−51.8	−33.1	−30	−29	−4.5	2.58	1478
		Ping13-2	1453.6–1483.2	E	1.07	68.85	26.43	3.55	−52.7	−33.2	−29.8	−29	−4.74	2.56	1220
		Ping13-4	1450.8–1486.4	E	1.21	74.92	19.04	4.26	−51.7	−33.2	−29.8	−28.6	−4.43	2.54	1722
		Ping14-3	1467–1484.6	E	0.61	77.93	18.17	3.15	−51.8	−33.2	−29.9	−29.1	−4.32	3.19	1378
		Bin4	1510–1568	E	/	60.72	32.62	4.91	−49.4	−32.4	−28.9	/	−9.8	/	/
		Bin1	1890–1898	E	/	94.13	3.53	2.09	−45.8	−30.1	−27.4	/	−6.1	/	/
		Bin11	1980.2–2250	E	/	97.32	1.31	1.06	−47.6	/	/	/	−5.9	/	/
	Pingnan	Bin4-6-41	/	E	/	63.17	36.83	/	−50.80	/	/	/	−6.68	1.372	/
		Bin12-X41	/	E	/	86.79	13.2	/	−49.65	/	/	/	−7.07	/	/
		PingG11-1	/	O	/	97	2.99	/	−50.10	/	/	/	−6.98	/	/
		PingN167	/	O	/	90.41	9.54	/	−48.62	/	/	/	−5.51	/	/
		BinG14-1	/	O	/	57.41	42.59	/	−47.45	/	/	/	−5.02	/	/
		BinG11	2229.0–2248.2	O	0.3	97.32	1.31	1.06	/	/	/	/	−5.9	/	/
		BinG14	1980.2–2250	O	0.46	96.99	1.16	1.39	−47.5	−32.1	−29.6	−28.6	−4.76	2	/
		BinG24	/	/	0.88	74.65	17.11	7.36	−46.4	−32.7	−29.9	−29	−4.64	3.73	/
	Gaoqing	Gao3	833.4–834.8	N	/	97.87	0.07	/	−4.41	−35	/	/	/	/	/
IV	Gaoqing	GaoQ10	824.3–838.9	N	/	99.99	0	/	−5.2	/	/	/	/	/	/
		GaoQ12	820–850	N	/	99.91	0.08	/	−7.7	/	/	/	/	/	/
		GaoQ3	833.4–834.8	N	5.43	94.35	0.14	0.08	−4.41	−35	/	/	/	4.47	/
		Gao53	811.4–818	N	/	99.96	0.04	/	−6.8	/	/	/	/	/	/
	Huagou	Hua17	1965.1–1980	E	1.6	93.78	3.89	0.63	−54.4	−33.2	−31.3	−29	−3.41	3.18	770
		Hua17	2000–2009.6	E	2.04	92.69	3.82	1.45	−54	/	−29.5	/	−3.35	3.21	1054
	Balipo	Yang25	2793.9–2805	E	3.06	96.5	0.44	/	−42.5	−25.7	/	/	−4.38	2.94	3000
		Yang2	2716–2760.8	O	0.06	98.59	1.35	/	/	/	/	/	/	/	
		Yang5	2611–2645.4	O	/	97.37	2.48	/	/	/	/	/	/	/	/

those confirming the carbon isotope threshold of coal-derived gas fall in zones I and V in Fig. 7. Group II gases from Wells Yi11-381, Yi11-G25, Yi17, and Yi171 had $\delta^{13}C_1$ values lower than −55‰, and the values of $\delta^{13}C_2$ were between −40‰ and −35‰, which falls in the VI zone, implying that these samples are biogas. However, these samples were wet gas, as their drying coefficient was lower than 0.90, indicating that the gases seem to be a mixture of thermogenic gas and biogas. Figure 8 provides further insight into the genetic types of the samples: some Group II gases from the Gudong Gas Filed had high C_1/C_{2+3} ratios that plot outside the boundary of the D zone in Fig. 8, while the rest fall well within the D and G zones, showing a typical pattern of oil-associated gas and coal-derived gas. For the samples that have high C_1/C_{2+3} ratios, most over 100, the identification diagram established by Bernard et al. (1978) can give the interpretation, as shown in Fig. 9, in which the samples' C_1/C_{2+3} ratios are higher than thermogenic gases and fall within the secondary transformation zone. This is compared with typical oil-associated gas, in which the $\delta^{13}C_1$ and $\delta^{13}C_2$ values are 3–8‰ heavier than those of oil-associated gas, and show the distribution of $\delta^{13}C_1 < \delta^{13}C_2 < \delta^{13}C_3 > \delta^{13}C_4$. Thus, it can be stated that the high C_1/C_{2+3} value is caused by secondary effects such as long-distance migration or biological action.

Oil-related gases include mature oil gas (oil-associated gas) and high-maturity oil gas. High-mature oil-related gas has high $\delta^{13}C_2$ and $\delta^{13}C_3$ values, and is commonly located near the boundary of the oil-associated gas zone

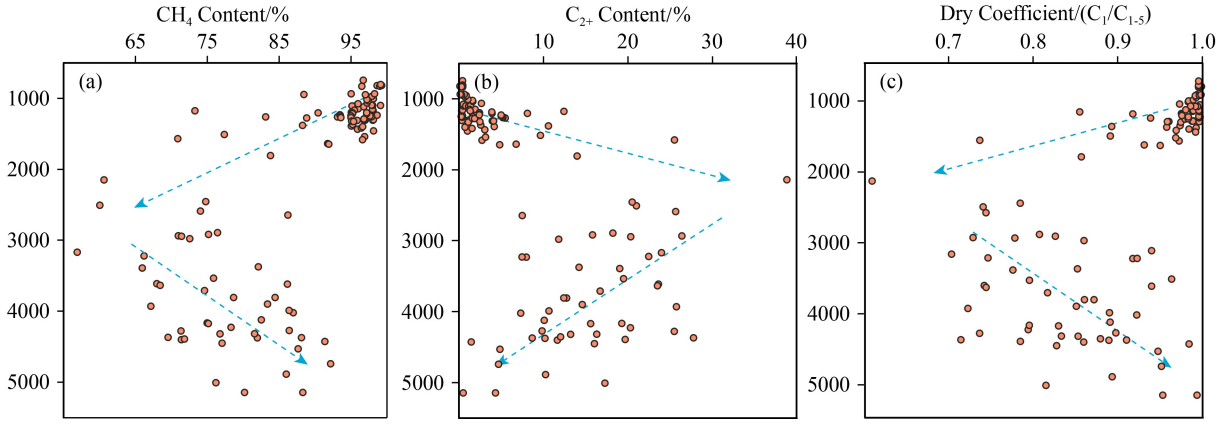

Fig. 3 Variation of CH_4 content, C_{2+} content and dry coefficient (C_1/C_{1-5}) of natural gases with depth in the Jiyang Depression.

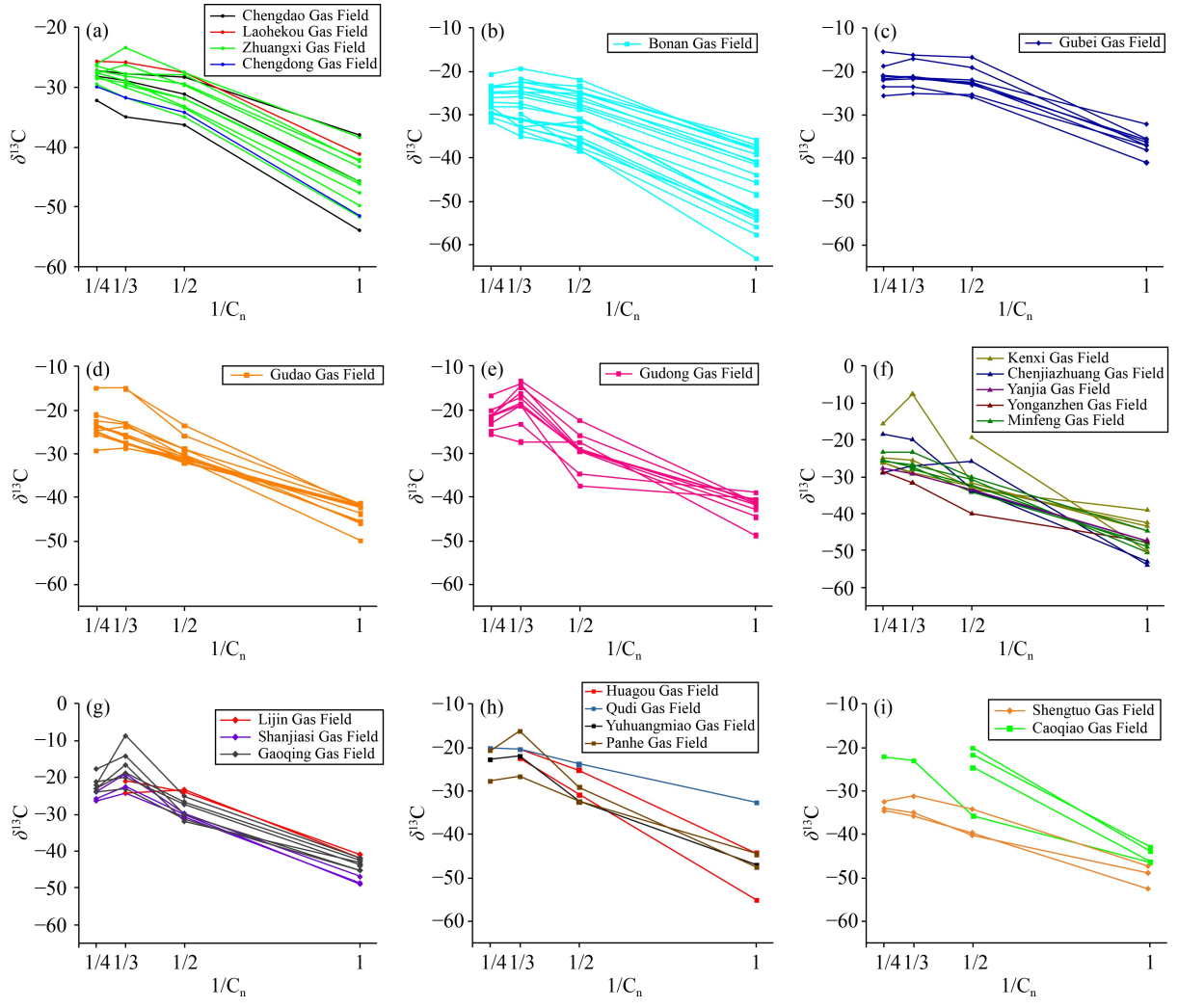

Fig. 4 Diagrams of $1/C_n$ versus $\delta^{13}C$ for natural gas samples in the Jiyang Depression. The linear, concave, and convex curves showing the relationship between $1/C_n$ and $\delta^{13}C$ indicate different origin of natural gas.

in Fig. 6. Using the differentiation chart (Fig. 10) proposed by Wang et al. (2009), it can be distinguished as to the genetic type of these samples, as shown in Fig. 10, the $\delta^{13}C_3$–$\delta^{13}C_2$ value of Group II gas from the Laohekou, Bonan (Wells BoS6, Bos601, BoS3) and Zhuangxi (Well ZhuangG23) Gas Fields varies from 10 to 15, while the $\delta^{13}C_1$ values are −45‰ to −35‰, plotting in zone III, which demonstrates a typical pattern of high-mature oil-related gas. In summary, the genetic types of Group II are very complex, except for non-inorganic gas,

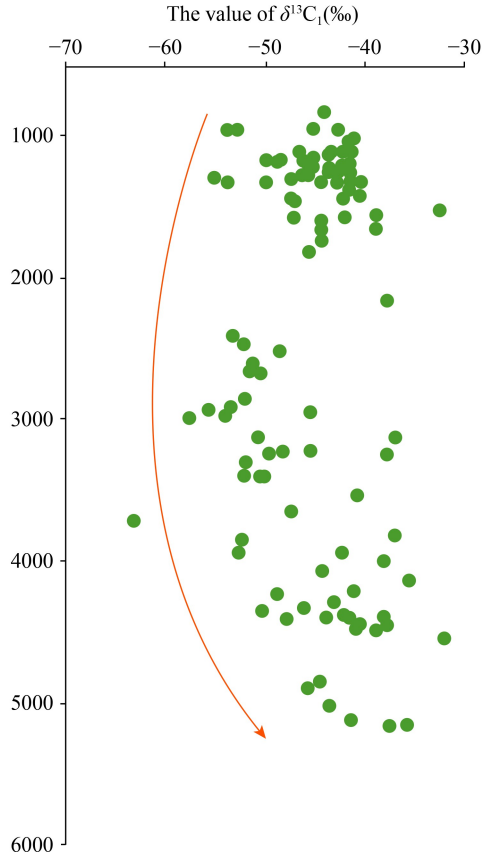

Fig. 5 Variation of $\delta^{13}C_1$ of hydrocarbon gases with depth in the Jiyang Depression.

and other genetic types of natural gas are all involved.

5.1.2 Genetic types of samples in south depression

For Group III, the geochemical characteristics of the samples are also complicated, and the $\delta^{13}C_2$ and $\delta^{13}C_3$ values were generally lower than those of Group II, but some samples had higher $\delta^{13}C_3$ values, up to −8.52‰. Biogas, whose $\delta^{13}C_1$ value is typically less than −55‰, was only distributed in the Huagou Gas Field. The samples from Guangli, Xianhe, and Liangjialou Gas Fields had high contents of C_{2+} components, and their drying coefficients were less than 0.95, which is typical of wet gas. Moreover, the values of $\delta^{13}C_1$ were between −55‰ and −50‰, which shows the characteristics of typical oil-associated gases. Samples from the Panhe area all conformed to the oil-associated gas boundary in Fig. 6 and fell into the zone II in Fig. 7 and zone D in Fig. 8. The samples from Caoqiao, Huagou, Gaoqing and Shanjiasi Gas Fields had shallow burial depth, and were significantly affected by secondary changes, as reflected in Fig. 9. The figure shows that their C_1/C_{2+3} and $\delta^{13}C_3$ values were very high and, all fell in the secondary transformation zone; moreover, the distribution of $\delta^{13}C_3 > \delta^{13}C_4$ further confirm this conclusion. The samples from Shengtuo and Lijin, whose burial depth was more than 4000 m, had a slightly higher dryness coefficient than the oil-associated gas in Xianhe and other areas. Their $\delta^{13}C_2$ and $\delta^{13}C_3$ values were located near the boundary of the oil-associated gas zone, and the $\delta^{13}C_3$–$\delta^{13}C_2$ values and $\delta^{13}C_1$ values fell within the range of high-mature oil-related gas zone in Fig. 10, which shows that they are typical high-maturity oil-associated gases. Although the natural gas from Minfeng was ever distinguished as kerogen cracking gas by a few samples (Luo et al., 2008; Hu et al., 2009), according to the judging chart (Fig. 11) proposed by Prinzhofer and Huc (1995), the variation trend of $\ln(C_2/C_3)$ and $\delta^{13}C_3$–$\delta^{13}C_2$ of the gas samples is more consistent with that of oil-cracked gas. In addition, the $\delta^{13}C_1$ value was lower than that of typical kerogen pyrolysis gas, so it can be determined that the gas samples in the Minfeng area are mainly oil-cracked gas, which is consistent with the conclusions of Li et al. (2010) and Yang et al. (2014).

In addition to the above hydrocarbon reservoirs, Group III also contain CO_2 gas samples from the Huagou, Pingfangwang, Pingnan Gas Fields. Further, it is known that the genetic type of CO_2 can be classified as inorganic or organic. Considering this, these samples had high $\delta^{13}C_{CO_2}$ values, most over −8‰, ranging from −9.8‰ to

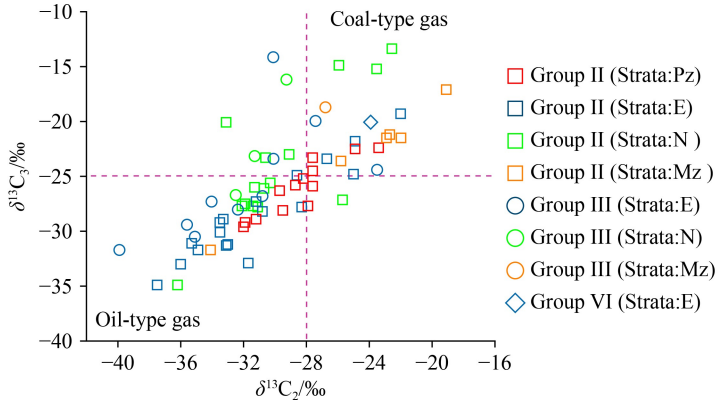

Fig. 6 The diagram of $\delta^{13}C_2$ versus $\delta^{13}C_3$ for oil-associated gas and coal-derived gas, most oil-associated gas displays lower $\delta^{13}C_2$ (< −28 ‰) and $\delta^{13}C_3$ (< −25 ‰) values than coal-derived gas.

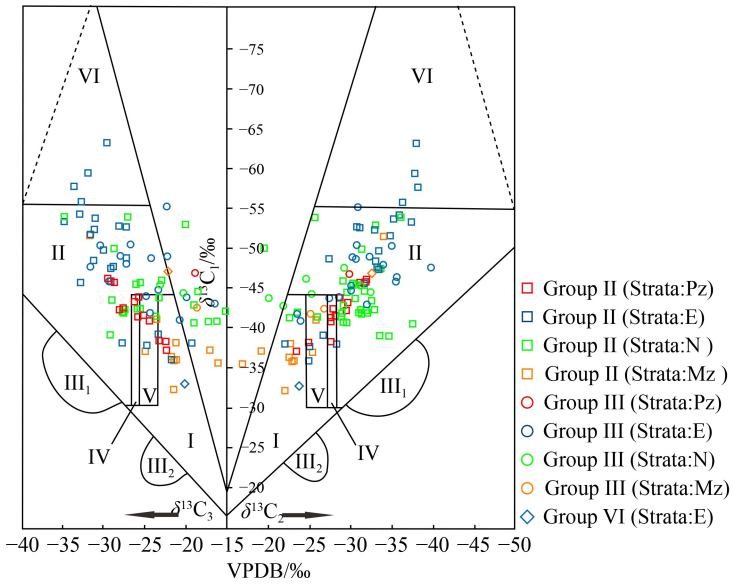

Fig. 7 Characteristics of $\delta^{13}C_1$, $\delta^{13}C_2$ and $\delta^{13}C_3$ in Jiyang Depression (modified after Dai et al., 1993), the different characteristics of different gas sample can indicate the type of it. Notes: I= coal-derived gas, II= oil-associated gas, III= carbon isotope series inversion gas, IV= coal-derived gas and oil-associated gas, V= coal-derived gas and oil-associated gas and combination gas, VI=biogas and sub-biogas.

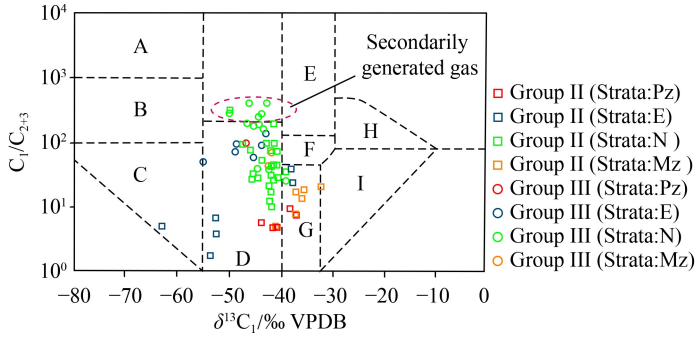

Fig. 8 Diagram showing C_1/C_{2+3} versus $\delta^{13}C_1$ for identification of oil-associated gas and other gases at different thermal evolution stages (modified after Dai et al., 1993). Notes: A= biogas, B= biogas and sub-biogas, C= sub-biogas, D= oil-associated gas, E= cracked gas, F= cracked gas and coal-derived gas, G= condensate associated gas and coal-derived gas, H= inorganic gas and coal-derived gas, I=coal-derived gas.

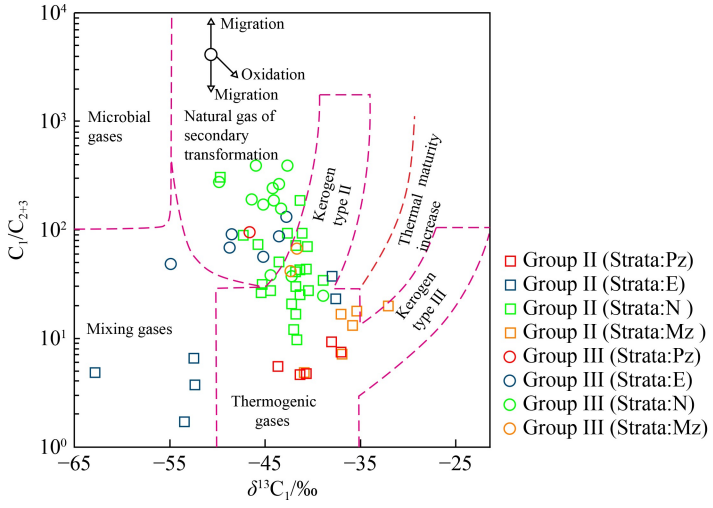

Fig. 9 The correlation diagram between $\delta^{13}C_1$ and $C_1/(C_2+C_3)$ (modified Bernard, 1976) for different types of natural gas in Jiyang Depression. Thermogenic gases display increasing $\delta^{13}C_1$ values and $C_1/(C_2+C_3)$ ratios with increasing thermal maturity. And natural gases of secondary transformation display higher $C_1/(C_2+C_3)$ values.

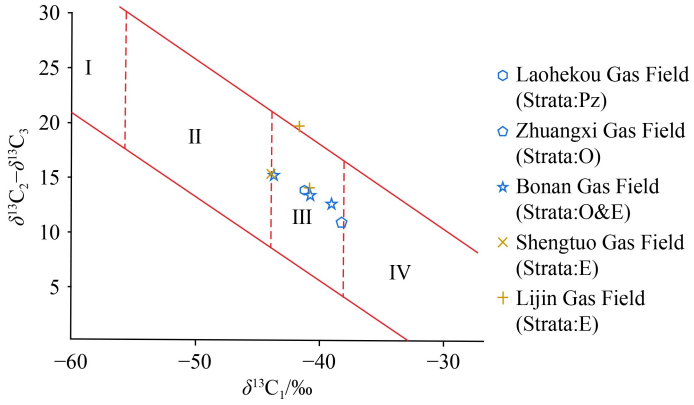

Fig. 10 The plot of $\delta^{13}C_2$–$\delta^{13}C_3$ versus $\delta^{13}C_1$ to discriminate the high mature oil-associated gases (modified after Wang et al., 2009). Using this diagram can eliminate the effects of too high carbon isotope to blurry the boundary of identification of natural gases in Jiyang Depression. Notes: I= biogas, II= oil-associated gas, III= high-mature oil-related gas, IV= coal-derived gas.

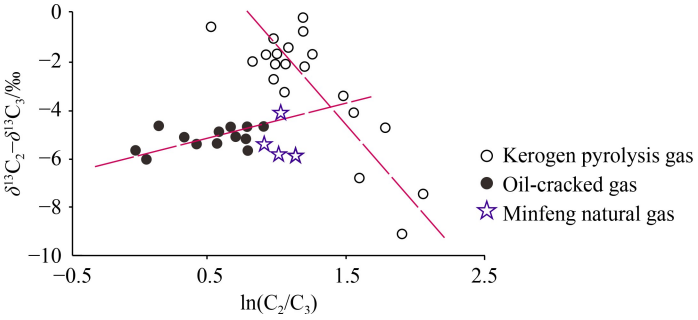

Fig. 11 The diagram of $\delta^{13}C_2$–$\delta^{13}C_3$ versus ln(C_2/C_3) values of different types of natural gas (modified after Prinzhofer et al., 1995). The data of kerogen pyrolysis gas is from California Gas Field. The data of oil-cracked gas is from Kansas Gas Field.

−3.35 ‰, indicating inorganic characteristics. The cross-plot of CO_2 content vs. $\delta^{13}C_{CO_2}$ also confirms that these samples are inorganic gas, as shown in Fig. 12 (Dai et al., 1992), in which all samples fall into zone II. Next, we consider that inorganic gas can be further divided into mantle-derived gas and crust-derived gas, which can provide meaningful information about the accumulation model of CO_2 reservoirs (Dai et al., 1992; Li et al., 2004; He et al., 2005a, 2005b). According to the relationship between $\delta^{13}C_{CO_2}$ and R/Ra, He et al. (2005a, 2005b) proposed an identification chart for inorganic CO_2 (Fig. 13). For this study, as shown in Fig. 13, the R/Ra values of most samples were higher than 2 and fell in the mantle-derived zone. In addition, their $^{40}Ar/^{36}Ar$ values were also relatively high, ranging from 317 to 3000, most of which were greater than 1000 (Table 3), revealing the characteristics of mantle-derived Ar.

For Group IV, as shown in Tables 2 and 3, the samples from the Yangxin Gas Field had low $\delta^{13}C_1$ value, ranging from −60.9 ‰ to −56.5 ‰ (av. −59.3 ‰), and a high drying coefficient (all over 0.99), showing a typical pattern of biogas. As shown in Fig. 7, the cross-plots of $\delta^{13}C_1$ versus $\delta^{13}C_2$ and $\delta^{13}C_3$ demonstrated that the samples from the Qudi and Yuhuangmiao Gas Fields fell into various regions. The former fells into zone I, showing coal-derived gas characteristics, while the latter fell into zone II, showing oil-associated gas characteristics. In addition, the CO_2 gas samples from the Balipo Gas Field had high R/Ra values, which fell into the volcanic mantle-derived inorganic CO_2 zone in Fig. 13.

It has been established that, based on the characteristics of natural gas components and carbon isotopes, natural gas samples can typically be divided into five types: oil-associated gas, high-mature oil-related gas, coal-derived gas, biogas, and secondarily generated gas, among which, the oil-associated gas is predominant. In this study, we find specifically that, Group I is the only oil-associated gas, while Group II has all genetic types, which are dominated by oil-associated gases. The gas samples from Group IV are mainly biogas, while Group III is largely oil-associated gas and high-mature oil-associated gas.

5.1.3 Distribution of gas genetic types

As shown for the distribution of natural gas genetic types in the Jiyang Depression (Fig. 14), the law of type changes from north to south and has two changing trends as follows. First, in the east, when reaching the Chenjiazhuang uplift, the complex types of gas changes to only oil-associated gas, and then the genetic types become complicated again. In the west, the changing trend of the genetic type of natural gas becomes gradually, increasingly complicated from north to south.

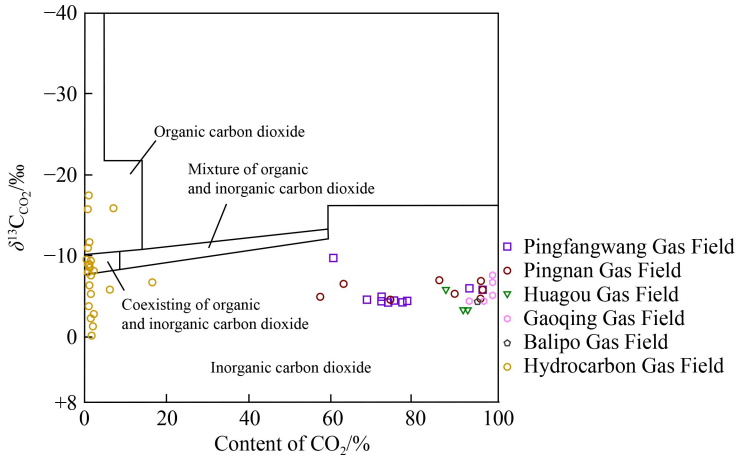

Fig. 12 Discrimination plot of CO_2 indicating the origin of CO_2 from the Jiyang Depression

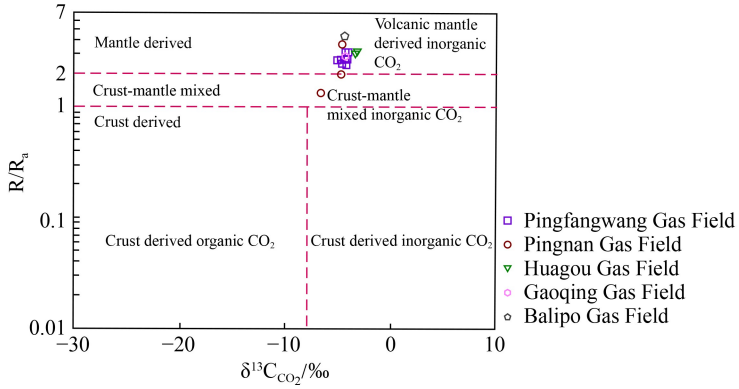

Fig. 13 Identifying origin of inorganic CO_2 chart according to $\delta^{13}C_{CO_2}$ and R/Ra value.

Furthermore, combining the genetic type of the gas reservoir with its burial depth (Fig. 15) reveals that the vertical distribution of natural gas in the Jiyang Depression has no obvious progressive change. Oil-associated gases are distributed in all layers, while high-mature oil-related gas is mainly distributed in deep layers, coal-derived gas is mainly distributed in the middle and deep layers, and the inorganic CO_2 gas reservoirs are mainly distributed in the middle and shallow layers.

According to the R_o calculation formulas in general for oil-associated gas: $\delta^{13}C_1 = 15.8\ \lg R_o - 42.2$ and $\delta^{13}C_1 = 21.72\ \lg R_o - 43.31$ and for coal-derived gas: $\delta^{13}C_1 = 14.12 \cdot \lg R_o - 34.39$ (Dai, 1993; Wang, 2008; Li et al., 2015), it is implied that the values of R_o do not increase with the increase in burial depth, which is confirmed by the findings of this study (Fig. 16). However, the samples also show that, in a certain depth range, incremental changes still occur. This indicates that in this study area, the vertical distribution of genetic types of natural gas is not only controlled by the maturity of the source rock, but also by other conditions such as tectonic evolution (Wang et al., 2017; Wu et al., 2017)

5.2 Main controlling factors for the occurrence of natural gas

5.2.1 Distribution of gas genetic types controlled by source rock conditions

Previous studies have demonstrated that the source rocks exert an important control on hydrocarbon accumulation and distribution (Guo et al., 2014; Liu et al., 2016b; Tian et al., 2018; Li et al., 2019b; Zhang et al., 2020). The spatio-temporal changes of gas reservoirs shown in Figs. 14 and 15 demonstrate that gas reservoirs in the Jiyang Depression are closely related to the qualities and thermal evolution of the source rocks. The source rocks in Jiyang Depression mainly include Paleogene E*s*, E*k*, and Upper Paleozoic Carboniferous–Permian strata.

The northwest area, where Group I gas is located, extending to the Yihezhuang Uplift in the east and the Chenjiazhuang Uplift in the south, belongs to lacustrine deposits. The main source rocks are Es_1, Es_3 and Es_4, and the main hydrocarbon-bearing strata are Paleogene strata. Although the Lower Paleozoic carbonate strata can also generate hydrocarbons, they are not the main source rocks. The results of this study show that the TOC value of Es_4 is between 1.0% and 8.0%, Es_3 is between 2.5%

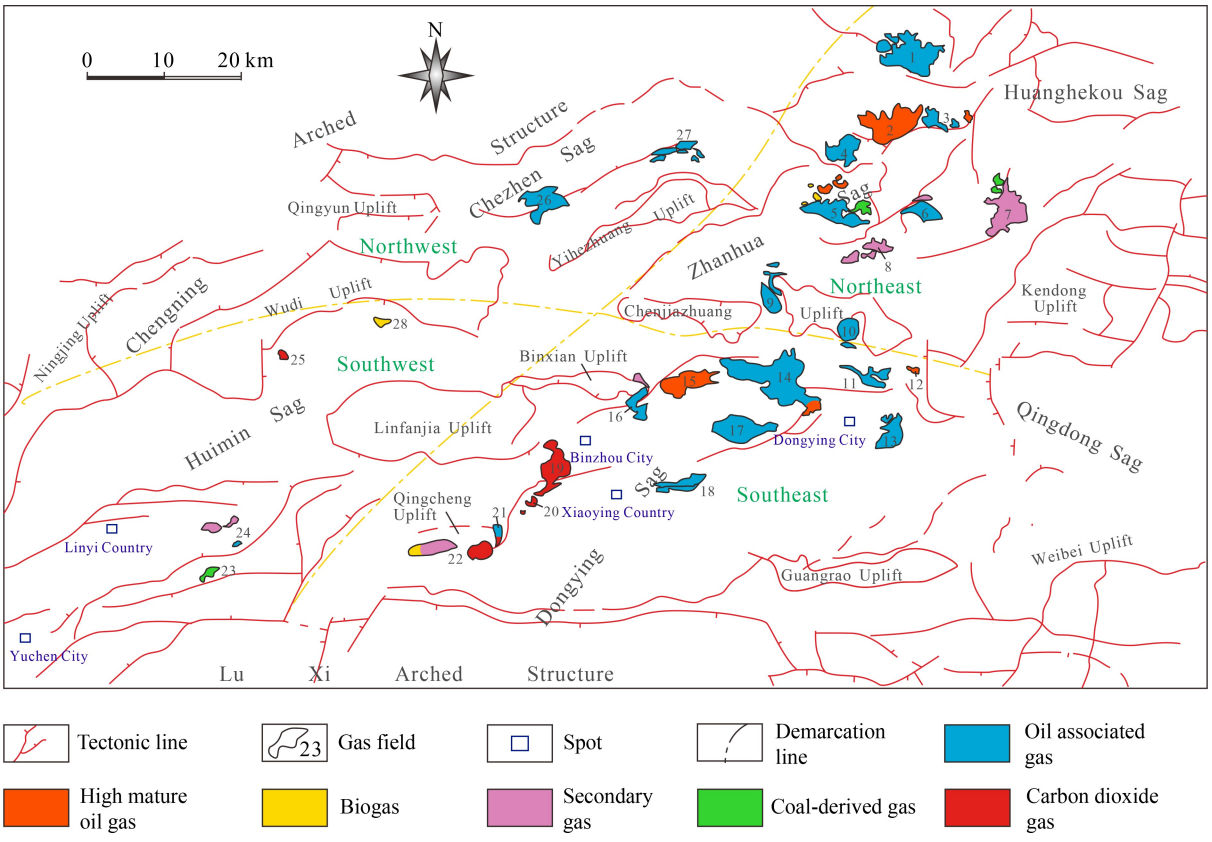

Fig. 14 Transverse distribution of different origin of natural gases reservoir in Jiyang Depression (Gas Fields: 1-Chengdao Gas Field, 2-Laohekou Gas Field, 3-Zhuangxi Gas Field, 4-Chengdong Gas Field, 5-Bonan-Gubei Gas Field, 6-Gudao Gas Field, 7-Gudong Gas Field, 8-Kenxi Gas Field, 9-Chenjiazhuang Gas Field, 10-Yanjia Gas Field, 11-Yonganzhen Gas Field, 12-Minfeng Gas Field, 13-Guangli Gas Field, 14-Shengtuo Gas Field, 15-Lijin Gas Field, 16-Shanjiasi Gas Field, 17-Xianhe Gas Field, 18-Liangjialou Gas Field, 19-Pingfangwang Gas Field, 20-Pingnan Gas Field, 21-Gaoqing Gas Field, 22-Huagou Gas Field, 23-Qudi Gas Field, 24-Yuhuangmiao Gas Field, 26-Dongfenggang Gas Field, 27-Dawangzhuang Gas Field, 28-Yangxin Gas Field).

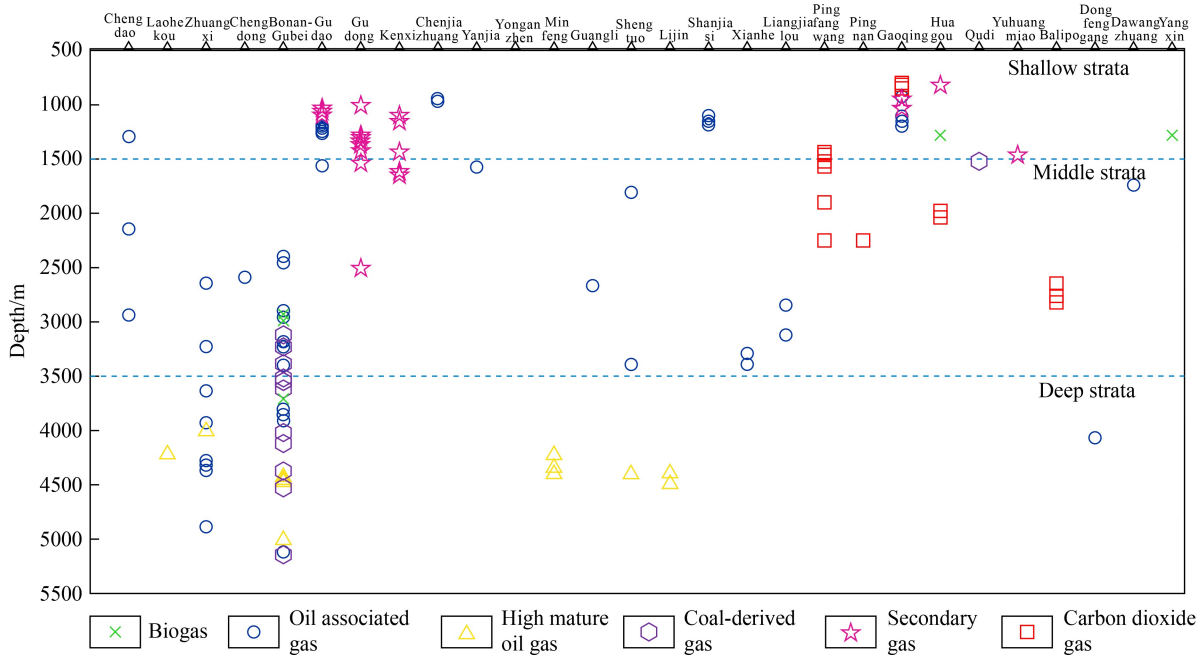

Fig. 15 Longitudinal distribution of different origin of natural gases reservoir in Jiyang Depression.

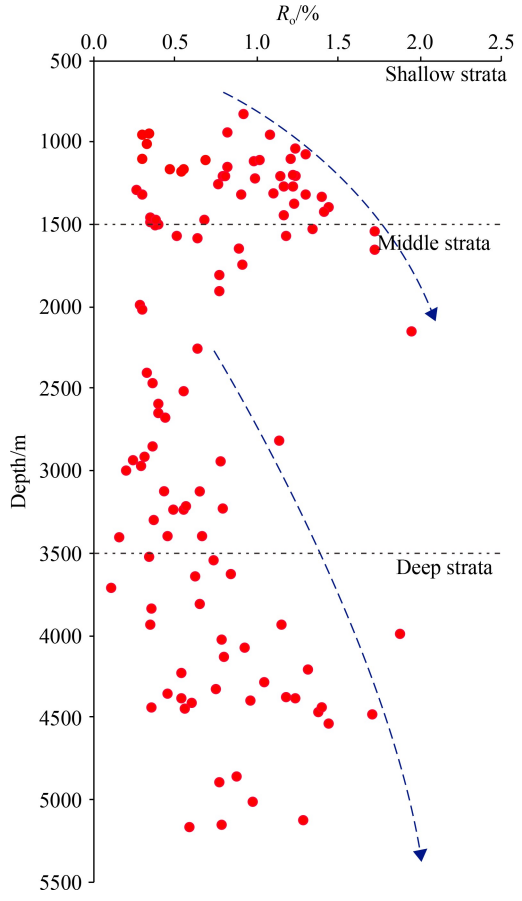

Fig. 16 Variation of R_o of natural gases with depth in the Jiyang Depression.

and 12.1%, and Es_1 is approximately 5.5%, implying that they are all excellent source rocks, and lay a material foundation for the generation of natural gas. The burial depths of Es_4 and Es_3 are greater than 3000 m, and the value of R_o is over 0.5%, indicating that they have entered the peak of hydrocarbon generation, with both Type I and Type II_1 kerogen, mainly producing oil and oil-associated gas. The Es_1 Formation is distributed throughout the entire area, but its burial depth is 1600–2800 m, the value of R_o < 0.5‰, in the immature stage, so it is not the main gas production unit. Carboniferous to Permian coal-measure strata is also distributed in this area, but the average thickness of the coal seam is very small, and its R_o value is low (Fig. 17), indicating that these strata have just entered the early mature stage without a large amount of hydrocarbon generation. Although the Mesozoic strata in the Jiyang Depression have a secondary hydrocarbon generation process during the Himalayan period, they were not found in this area. Therefore, only oil-associated gas reservoirs are found in this area.

The northeast area, where Group II gas is distributed and which is bordered by the Yihezhuang Uplift in the west and the Chenjiazhuang Uplift in the south, includes many oil-rich subsags, for example, Bonan subsag. Compared with the northwest area, except for Es_1, Es_3, and Es_4, the Carboniferous–Permian coal measure strata are also the main source rock. The Es_4^1 in this area has a high TOC value (ranging 0.77% to 15.18%), and a burial depth of up to 5200 m, corresponding to a high value of Ro (between 0.8% and 1.56 ‰), implying that it is in the high-mature stage and in the oil generation-condensate

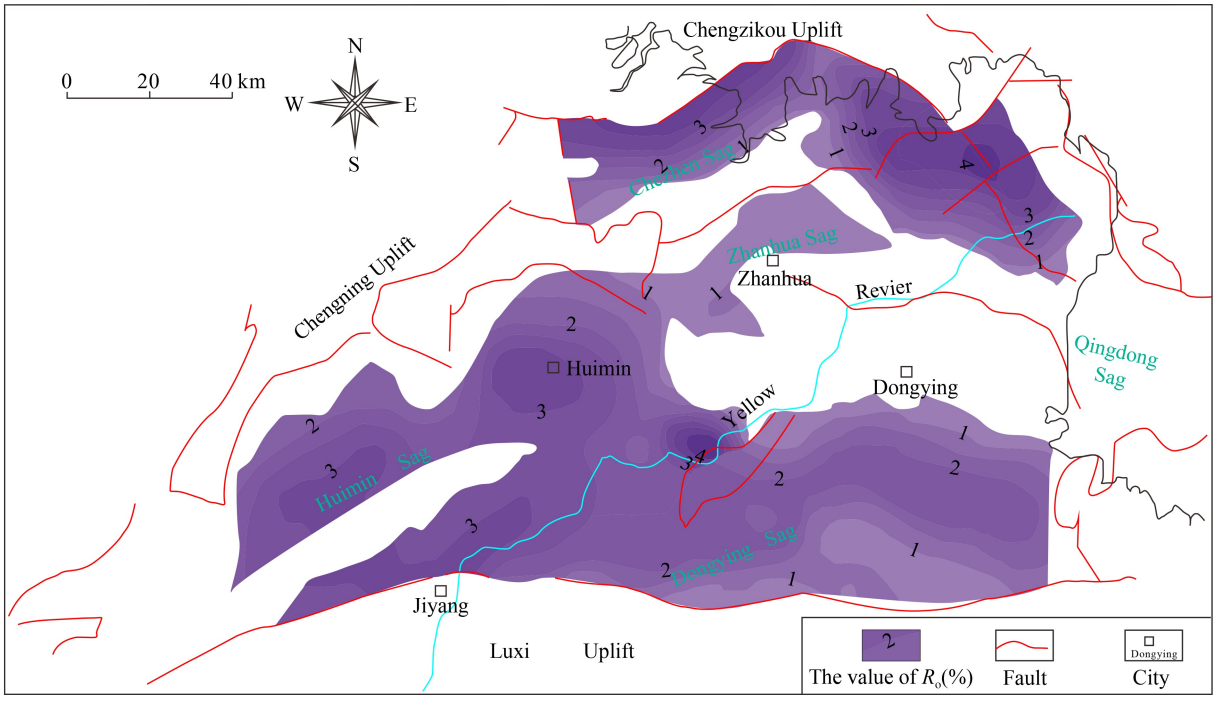

Fig. 17 The distribution of Carboniferous–Permian strata and contour map of its R_o value.

stage. It produces high-mature oil-related gases. The characteristics of Es_3 in this area are similar to those of Es_3 in the northwest, the corresponding TOC values are between 0.55% and 12.44%, and the main OM is Type I and Type II_1. Its R_o value ranges from 0.64% to 1.12%, inferring that it is a mature source rock that mainly generates oil-associated gas. The coal-derived gas is mainly produced by the Carboniferous–Permian coal measure strata in the Bonan-Gubei area, which is mainly distributed in the buried hill area (Fig. 17). The thickness of the coal seam is approximately 30 m, and the R_o value is between 0.94% and 1.77%, indicating that it is a mature source rock, which is conducive to a large amount of gas generation. Moreover, it is thought to have two hydrocarbon generation processes, the first hydrocarbon generation period being at the end of the Middle Triassic, and the second being in the Yanshanian–Hishanian Period (Wang et al., 2010; Zhu et al., 2010). Typically, since the first generation of hydrocarbons is difficult to preserve through tectonic evolution, the gas generated by the second generation of hydrocarbons can form gas reservoirs, and has higher research value. The biogas in this area was mainly generated from Es_1. The corresponding TOC value was between 0.9% and 7.0%, and the OM was Type I, the buried depth was less than 3000 m, and the R_o was between 0.43% and 0.60%, implying that it is in the immature stage, generating biogas reservoirs. In addition, the shallow biological action in this area is relatively strong, which is another main reason for the formation of the biogas reservoirs.

In the southeast area, where Group III gas is distributed, the main source rocks in this area are Es_4 and Es_3. In recent years, studies have determined that the second member of the E*k* Formation has a certain hydrocarbon expulsion potential, but it is not the main source rock (Ren et al., 2006; Chen et al., 2011). The burial depths of Es_3 and Es_4^1 are relatively shallow (between 2000 and 3000 m) corresponding to the R_o value ranging from 0.58% to 1.03% and their OM is mainly Type I and Type II_1 mixed with a small amount of kerogen II_2, indicating that they mainly produce oil-associated gas reservoirs. The oil-cracked gas mainly comes from the lower subsection of Es_4, which belongs to salt-lake sediment, and its burial depth is more than 4200 m in the Minfeng area, with the ground temperature exceeding 160°C, showing that it has the conditions for cracking crude oil into gas. The Carboniferous–Permian strata are also distributed in this area, and the thickness of the coal measure is approximately 20 m, which has the potential for hydrocarbon generation. However, the hydrocarbon generation process was mainly in the Indosinian movement, and the natural gas reservoirs that were generated at this time were difficult to preserve after structural changes. After the Yanshanian and Himalayan Periods, the ground temperature increased with increasing the burial depth, but the secondary hydrocarbon generation process was not found in this area (Fan et al., 2008; Wang et al., 2010). Owing to the influence of strong volcanic movement, it is not easy to generate large-scale gas reservoirs, so no coal-derived gas reservoirs are distributed in this area.

The southernmost part of this area is the Huagou and Gaoqing Gas Fields, which are connected to the Qingchengshan Uplift in the north. This area contains both CO_2 gas reservoirs and hydrocarbon gas reservoirs. The CO_2 gas reservoir is of volcanic mantle origin, which is related to the development of multiple magma eruptions. The main source rocks of the hydrocarbon gas reservoirs in this area are Es_1 and Es_3. The burial depth of Es_3 is between 1800 and 3500 m and the corresponding R_o value is between 0.36% and 0.8%, indicating that it mainly produces oil-associated gas. Meanwhile, the R_o value of Es_1 is < 0.5%, which is in the immature stage and generates biogas reservoirs.

The southwest area, where Group IV gas is distributed and whose source rocks are also Es_4 and Es_3, reaches to the Wudi Uplift in the north and Linfanjia Uplift in the east. The TOC value of them is about 3%, the burial depth is approximately 3000 m, and the R_o value is greater than 0.65%, indicating the early mature stage, while the OM is mainly Type I and Type II_1, generating oil-associated gas reservoirs. The main characteristic of this area is the coal-derived gas reservoirs in the Qudi area. In the buried hill zone of the Qudi area, the Upper Paleozoic Carboniferous–Permian coal-measure strata are rich in coal resources (Fig. 17), the thickness of the coal seam is large, and the OM type is Type III, which is conducive to gas generation. According to the history of hydrocarbon generation, the Carboniferous–Permian strata experienced two peaks of hydrocarbon generation after the deposition of the Early Triassic and the Jurassic to the Cretaceous. In addition, the Qudi buried hill area is close to the secondary gas generation center with sufficient gas injection. Reservoir types include sandstone, carbonate rock and igneous rock, all of which perform good storage conditions, so coal-derived gas reservoirs can be generated. The Yangxin subsag is located in the northeast part of this area. Biogas reservoirs are also distributed in this area, primarily due to the relatively well-developed bio-limestone in the Es_1 formation, and its shallow burial depth (approximately 1750 m), low thermal evolution (the R_o value is less than 0.4%).

In general, by summarizing the source rock characteristics of each part (Table 2), it is demonstrated that the lateral distribution of various genetic types of natural gas in the Jiyang Depression is controlled by the characteristics and distribution of the Es_1, Es_3, Es_4 and Carboniferous–Permian coal-measure strata. To further explore and develop certain types of natural gas in the Jiyang Depression, future research should look for potential zones based on the distribution of these source rocks.

5.2.2 Distribution of gas genetic types controlled by tectonic conditions

Tectonic conditions in general refer to various transport systems and tectonic movements in various periods that affect the formation of natural gas reservoirs (Zhang, 2012; Li et al., 2021b). They also play a decisive role in the distribution of various types of gas reservoirs, especially with regard to the vertical distribution.

In the Jiyang Depression, it has been established that tectonic conditions control the thickness and distribution of source rocks, thereby affecting the distribution of gas reservoirs (Wu, 2018; Chen, 2019). According to the occurrence of faults, fault regions can be divided into three groups: NE-, NW-, and near-E trending. The number and location of faults are well correlated with the thickness of the source rocks (Fig. 18). As shown in Fig. 18, source rocks are mainly distributed near active concave-controlling faults, and faults clearly control the extent of source rocks, that is, Es_3 extends along the NE direction and Es_4 is distributed in two directions along the NE and NW directions.

It is known that faults' sealing ability controls the process and the model of gas accumulation, hence for the study area it can be said as follow. 1) The biogas that was distributed in the mid-deep layer in the Bonan area was formed when the shallow biogas was transported to the middle layer under the favorable transportation condition of the Guxi fault. Some samples in this area are mixed sources that are inseparable from the development of multistage unconformities and good lateral migration channels. 2) The distribution of shallow gas reservoirs is directly related to tectonic conditions. Most shallow gas reservoirs are developed in the Neogene Minghuazhen Formation (N*m*) and Guantao Formation (N*g*). One of the factors for this is that those areas have good migration conditions in which many faults can communicate with the lower source rocks E*s*. The convex shallow gas accumulation model in the Gudao-Gudong area is a coincident example (Cheng et al., 1995). Another factor is that following the late Tertiary, the activity rate of faults had been very low, so the damage to the caprock was slight, which is conducive to the migration and accumulation of natural gas. 3) The distribution of coal-derived gas reservoirs is related to the secondary hydrocarbon generation of the Carboniferous–Permian strata, in which the evolution of tectonic activity determines its process. At the end of the Indosinian period, the first hydrocarbon generation stopped owing to the uplift of the depression. Reaching the rapid subsidence stage of the Yanshanian–Himalayan Period, the burial depth of the Carboniferous–Permian strata continued to increase, and the strata was affected by thermal anomalies, so the second hydrocarbon generation was initiated (Wang et al., 2010; Zhu et al., 2010). Because it is limited by the distribution of subsidence centers, secondary hydrocarbon generation was generated only in the northeast and southwest areas, and coal-derived gas reservoirs were only distributed in these two areas.

The finding shows that the distribution of inorganic CO_2 gas reservoirs in the study area is mainly affected by tectonic conditions. For example, in the southern area, which has undergone been multiple periods of magmatic activity since the Mesozoic and Cenozoic, the Balibo, Gaoqing, and Huagou Gas Fields are comprised of tertiary alkaline basalts located in this area. These alkaline basalts are facies conducive to the release of CO_2, and they provide a good material basis for the accumulation of CO_2 gas reservoirs (Shen et al., 2007; Hu et al., 2009; Wang et al., 2018). In general, it is understood that mantle-derived CO_2 gas generation requires deep connections to transport CO_2 in the mantle. The Tanlu Fault is the only fault that connects to the upper mantle lithosphere in the Jiyang Depression, thus mantle-derived CO_2 gas can be transported through it. In this area, only the Yangxin and Shicun Faults in the south connect the Tanlu Fault, and the Linshang, Xiakou, and Gaoqing-Pingnan Faults in the southern area have large cutting depths, which are also favorable channels for the transport of deep CO_2. Therefore, in the southern region, CO_2 gas reservoirs are mostly distributed at the intersection of the NE-, E-, and NW-trending faults (Fig. 19). In summary, the CO_2 gas reservoirs which are further favorable exploration targets are those representing structural and lithological traps near the fault zone in the southern area.

6 Conclusions

The hydrocarbon gas in the Jiyang Depression can be divided into four groups. Group I gas distributed in the northwest is only oil-associated gas. Group II gas distributed in the northeast area, is dominated by oil-associated gas, and involves biogas, coal-derived gas, and high-mature oil-relate gas. Group III, distribute in southeast area, has all genetic types gas and that also dominated by oil-associated gas, samples from the shallow layer have high $\delta^{13}C_3$ values, showing the distribution of $\delta^{13}C_1 < \delta^{13}C_2 < \delta^{13}C_3 > \delta^{13}C_4$. And Group III also contains volcanic mantle-derived carbon dioxide gas. Group IV gas distributed in the southwest area, is dominated by biogas and involves coal-derived gas and oil-associated gas. In short, natural gas samples in the eastern and southern depressions have more genetic types. However, in the vertical direction, the distribution of natural gas does not have an obvious evolutionary law.

There are two main factors controlling factors of the spatiotemporal changes of gas are in two aspects. First, the characteristics of the Shahejie Formation and Carboniferous Permian source rocks are various in different area. The occurrence of oil-associated gas reservoirs is mainly controlled by the maturity of Es_1, Es_3, and Es_4 and its burial depth. Second, the tectonic conditions, mainly the sealing properties of various faults, affected the lateral and

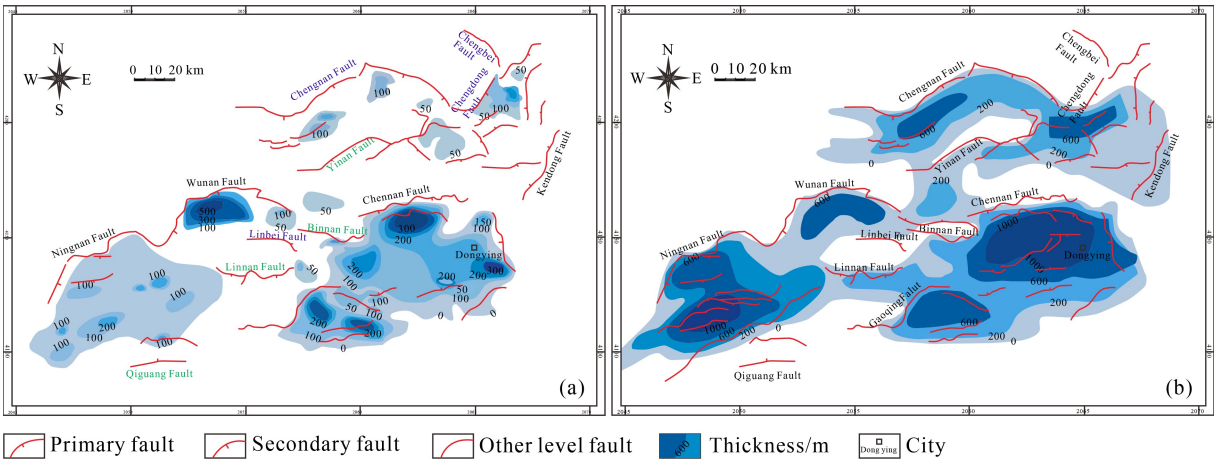

Fig. 18 Horizontal distribution of (a) Es_4 and (b) Es_3 in Jiyang Depression.

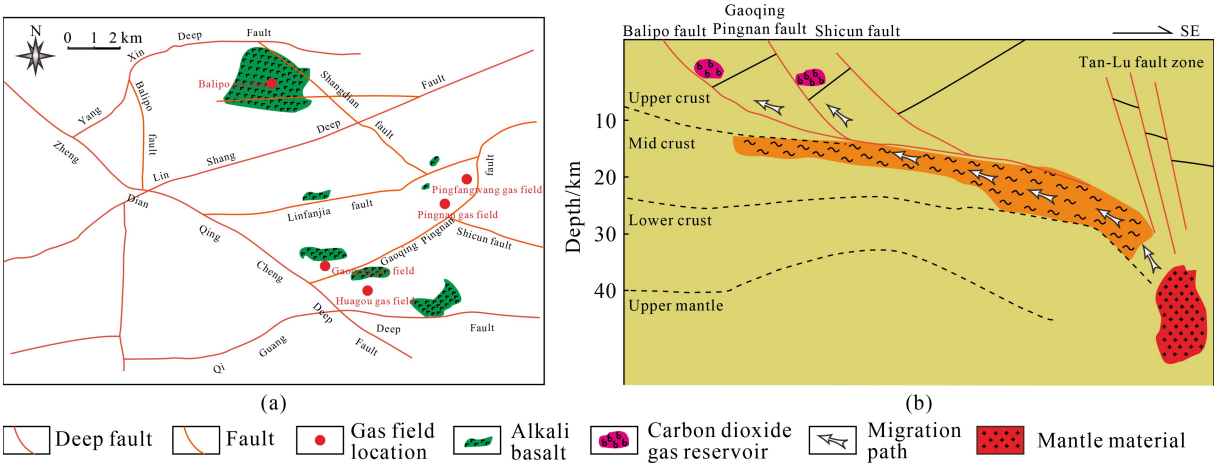

Fig. 19 (a) Distribution of CO_2 gas reservoir in Jiyang Depression and (b) accumulation model of CO_2 gas reservoir in Jiyang Depression.

vertical migration of hydrocarbon gases and the upwelling of mantle-derived CO_2. Moreover, the secondary hydrocarbon generation process of Carboniferous Permian is controlled by the uplift of strata, which has affected affecting the lateral distribution of coal-derived gas reservoirs. In general, the main controlling factor analysis of the spatiotemporal changes of gas reservoirs revealed that the synergy of characteristics, thermal evolution of the Shahejie Formation and Carboniferous–Permian source rocks, and sealing properties of various faults are jointly responsible for determining the spatiotemporal changes of gas reservoirs.

Acknowledgments This study was supported by the National Natural Science Foundation of China (Grant Nos. 42072172 and 41772120), the Shandong Province Natural Science Fund for Distinguished Young Scholars (No. JQ201311), and the Graduate Scientific and Technological Innovation Project Financially Supported by Shandong University of Science and Technology (No. SDKDYC190313). We thank Shengli Oil Company for providing samples and analysis data. The authors are also grateful for the critical comments and helpful suggestions raised by Associate Editor and anonymous reviewers, which greatly improved the quality of our manuscript.

References

Bernard B B, Brooks J M, Sackett W M (1978). Light hydrocarbons in recent texas continental shelf and slope sediments. J Geophys Res, 83(C8): 4053–4061

Cai C, Hu W, Worden R H (2001). Thermochemical sulphate reduction in Cambro–Ordovician carbonates in Central Tarim. Mar Pet Geol, 18(6): 729–741

Cai Y (2008). Characteristics of fault developed in Jiyang Sag and its control over hydrocarbon migration and accumulation. Nat Gas Geosci, 19(01): 56−61 (in Chinese)

Cao Z, Zhang Y, Cai P, Li Y, Liu J, Dong Y (2016). New achievements and recognitions of fine exploration in Jiyang Depression. China Petrol Explor, 21(03): 14−23 (in Chinese)

Ci X, Zhang H, Niu Q, Zhu D, Kang S, Hu J, Zhang L, Zhang J, He K (2020). Analysis of tight oil and gas charging characteristics by the carbon isotope on-site detection technology: a case study of the northern slope of the Minfeng Sub-sag in the Bohai Bay Basin. Nat Gas Indust B, 7(3): 197–204

Chen D, Pang X, Jiang Z, Zeng J, Qiu N, Li M (2009). Reservoir characteristics and their effects on hydrocarbon accumulation in lacustrine turbidites in the Jiyang Super-depression, Bohai Bay

Basin, China. Mar Pet Geol, 26(2): 149–162

Chen L (2019). Influence of fault activity on hydrocarbon accumulation in Jiyang Depression in the Cenozoic. Dissertation for Master's Degree. Qingdao: China University of Petroleum (in Chinese)

Chen J, Wang X, Ni Y, Xiang B, Liao F, Liao J, Zhao C (2019). Genetic type and source of natural gas in the southern margin of Junggar Basin, NW China. Pet Explor Dev, 46(3): 482–495

Chen T, Luo R, Wang J (2011). The geochemical characteristics of Shahejie Formation and Kongdian Formation hydrocarbon source rocks in the Jiyang Depression. J Chongqing U Sci Techn (Nat Sci Ed), 13(06): 23−25 (in Chinese)

Cheng Y, Song L, Guo J, Wang H (1995). Favorable conditions for shallow (Neogene) gas accumulation in Jiyang Depression. Pet Explor Dev, 22(16): 16−19 (in Chinese)

Clayton C (1991). Carbon isotope fractionation during natural gas generation from kerogen. Mar Pet Geol, 8(2): 232–240

Dai J (1990). A brief discussion on the problem of the geneses of the carbon isotopic series reversal in organogenic alkane gases. Nat Gas Indust, 10(06): 15−20+6 (in Chinese)

Dai J (1992). Indentification of various genetic natural gases. China Offshore Oil Gas, 6(01): 11−19 (in Chinese)

Dai J, Wen H, Song Y (1992). Natural gas of the mantle origin in Wudalianchi. Petrol Geo Exper , 14(02): 200−203 (in Chinese)

Dai J (1993). The carbon and hydrogen isotope characteristics and identify of different kinds of natural gases. Nat Gas Geosci, 2(3): 1−40 (in Chinese)

Dai J, Xia X, Qin S, Zhao J (2004). Origins of partially reversed alkane δ^{13}C values for biogenic gases in China. Org Geochem, 35(4): 405–411

Dai J, Li J, Luo X, Zhang W, Hu G, Ma C, Guo J, Ge S (2005). Stable carbon isotope compositions and source rock geochemistry of the giant gas accumulations in the Ordos Basin, China. Org Geochem, 36(12): 1617–1635

Dai J, Ni Y, Zou C (2012). Stable carbon and hydrogen isotopes of natural gases sourced from the Xujiahe Formation in the Sichuan Basin, China. Org Geochem, 43: 103–111

Dai J, Gong D, Ni Y, Huang S, Wu W (2014). Stable carbon isotopes of coal-derived gases sourced from the Mesozoic coal measures in China. Org Geochem, 74: 123–142

Dai J, Ni Y, Huang S, Gong D, Liu D, Feng Z, Peng W, Han W (2016). Secondary origin of negative carbon isotopic series in natural gas. J Nat Gas Geosci, 1(1): 1–7

Fan K, Zhang L, Zhou X, Huang C (2008). Hydrocarbon generation and evolution characteristics of Upper Paleozic source rock in Jiyang Depression. Mar Origin Petrol Geo, 13(1): 25−32 (in Chinese)

Gan Z, Yang X, Guo J, Xu Q (2005). Primary factors controlling gas reservoir forming in Jiyang Depression. Nat Gas Explor Develop, 28(3): 34−39+3 (in Chinese)

Gao C, Zhang Y, Wang X (2020). Genesis and source of shallow natural gas in the Jiyang Depression of the Bohai Bay Basin, Nat Gas Indust, 40(5): 26−33 (in Chinese)

Guo C, Shen Z, Yang G, Chen,Y, Luo X (2009). Geochemical characteristics and genetic classification of the natural gas in Gubei buried hill, Jiyang Depression, China. J Chengdu U Techn (Sci Techn Ed), 36(3): 231−237 (in Chinese)

Guo Z, Sun P, Li J, Zhang L, Liu W, Tian J, Zhang S, Zeng X (2014). Natural gas types, distribution controlling factors, and future exploration in the western Qaidam Basin. Acta Geol Sin, 88(4): 1214–1226

Hao F, Guo T, Zhu Y, Cai X, Zou H, Li P (2008). Evidence for multiple stages of oil cracking and thermochemical sulfate reduction in the Puguang Gas Field, Sichuan Basin, China. AAPG Bull, 92(5): 611–637

He J, Xia B, Wang Z, Liu B, Sun D (2005a). CO_2 migration rule from various origin and prediction of CO_2 favorable abundance zone in eastern China and offshore shelf basin. Nat Gas Geosci, 16(5): 622−631 (in Chinese)

He J, Xia B, Liu B, Zhang S (2005b). Origin migration and accumulation of CO_2 in east China and offshore shelf basins. Pet Explor Dev, 32(4): 42-49 (in Chinese)

Hu A, Dai J, Yang C, Zhou Q, Ni Y (2009). Geochemical characteristics and distribution of CO_2 gas fields in Bohai Bay Basin. Pet Explor Dev, 36(2): 181−189 (in Chinese)

Hu T, Pang X, Jiang F, Wang Q, Wu G Y, Liu X H, Jiang S, Li C R, Xu T W, Chen Y Y (2021a). Key factors controlling shale oil enrichment in saline lacustrine rift basin: implications from two shale oil wells in Dongpu Depression, Bohai Bay Basin. Petrol Sci, 18: 687–711

Hu T, Pang X, Jiang F, Wang Q, Liu X, Wang Z, Jiang S, Wu G, Li C, Xu T, Li M, Yu J, Zhang C (2021b). Movable oil content evaluation of lacustrine organic-rich shales: methods and a novel quantitative evaluation model. Earth Sci Rev, 214: 103545

Hu T, Pang X, Jiang S, Wang Q, Zheng X, Ding X, Zhao Y, Zhu C, Li H (2018). Oil content evaluation of lacustrine organic-rich shale with strong heterogeneity: a case study of the Middle Permian Lucaogou Formation in Jimusaer Sag, Junggar Basin, NW China. Fuel, 221: 196–205

Jiang Y, Liu H, Li Z (2009). Timing of deep gas accumulation in Bonan and Gubei areas of Jiyang Depression. Nat Gas Geosci, 20(5): 678−682 (in Chinese)

Jiang Y, Liu H, Li Z (2010). Effective migration pathways of deep gas in Bonan and Gubei area, Jiyang Depression. Geol Rev, 56(04): 525−530 (in Chinese)

Li C, Fan T, Zheng H (2004). Formation mode of carbon dioxide gas reservoirs in Yangxin-Huagou area. Acta Petrol Sin, 25(01): 35−40 (in Chinese)

Li H, Shahbaz M, Jiang H, Dong K (2021a). Is natural gas consumption mitigating air pollution? Fresh evidence from national and regional analysis in China. Sustain Product Consumpt, 27: 325–336

Li J, Hu G, Zhang Y, Yang G, Cui H, Cao H, Hu X (2008). Study and application of carbon isotope fractionation during the reduction process from CO_2 to CH_4. Earth Sci Front, 15(05): 357−363 (in Chinese)

Li J, Wang X, Wei G, Yang W, Xie Z, Li Z, Guo J, Wang Y, Ma W, Li J, Hao A (2018). New progress in basic natural gas geological theories and future exploration targets in China. Nat Gas Indust, 38(04): 37−45 (in Chinese)

Li J, She Y, Gao Y, Li M, Yang G, Shi Y (2020). Natural gas industry in China: development situation and prospect. Nat Gas Indust B, 7(6): 604–613

Li P, Jin Z, Zhang S, Pang X, Xiao H, Jiang Z (2003). The present research status and progress of petroleum exploration in the Jiyang Depression. Pet Explor Dev, 30(3): 1−4 (in Chinese)

Li W, Gao Y, Geng C (2015). Genetic types and geochemical

characteristics of natural gases in the Jiyang Depression, China. Petrol Sci, 12(1): 81–95

Li X, Li W, Zhang H (2005). Cracking gas reservoir-forming analysis and exploration orientation in Jiyang Depression. Petrol Geo Recover Efficienc, 12(1): 42−43+45−85 (in Chinese)

Li Y, Zhang J, Xu Y, Chen T, Liu J (2021b). Improved understanding of the origin and accumulation of hydrocarbons from multiple source rocks in the Lishui Sag: insights from statistical methods, gold tube pyrolysis and basin modeling. Mar Pet Geol, 134: 105361

Li Y, Chang X, Zhang J, Xu Y, Gao D (2019a). Genetic mechanism of heavy oil in the Carboniferous volcanic reservoirs of the eastern Chepaizi Uplift, Junggar Basin. Arab J Geosci, 12(21): 648

Li Y, Zhang J, Liu Y, Shen W, Chang X, Sun Z, Xu G (2019b). Organic geochemistry, distribution and hydrocarbon potential of source rocks in the Paleocene, Lishui Sag, East China Sea Shelf Basin. Mar Pet Geol, 107: 382–396

Li Y, Cha M, Gao C, Wang X, Zhang Y, Cui W, Wang Y (2017). The origin of shallow-buried natural gas in Sanhecun Sag, Jiyang Depression. J China U Min Techn, 46(02): 388–396

Li Y, Song G, Li W, Guo R, Yang X, Chen Y, Luo W (2010). A fossil oil-reservoir and the gas origin in the Lower Sha4 Member of the Well Fengshen-1 area, the north Dongying zone of the Jiyang Depression. Oil Gas Geo, 31(2): 173–179

Lin W, Li Z, Li J, Xu X (2007). Genetic types and distribution pattern of natural gases in Gubei Buried-hills, Jiyang Depression. Oil Gas Geo, 28(3): 419−426 (in Chinese)

Liu Q, Wu X, Wang X, Jin Z, Zhu D, Meng Q, Huang S, Liu J, Fu Q (2019). Carbon and hydrogen isotopes of methane, ethane, and propane: a review of genetic identification of natural gas. Earth Sci Rev, 190: 247–272

Liu Q, Jin Z, Li H, Wu X, Tao X, Zhu D, Meng Q (2018). Geochemistry characteristics and genetic types of natural gas in central part of the Tarim Basin, NW China. Mar Pet Geol, 89: 91–105

Liu Q, Dai J, Jin Z, Li J, Wu X, Meng Q, Yang C, Zhou Q, Feng Z, Zhu D (2016a). Abnormal carbon and hydrogen isotopes of alkane gases from the Qingshen gas field, Songliao Basin, China, suggesting abiogenic alkanes? J Asian Earth Sci, 115: 285−297

Liu X, Jiang Y, Hou Y, Liu J, Wen C, Zhu R, Wang F (2016b). Origins of natural gas and the main controlling factors of gas accumulation in the Middle Ordovician assemblages in Jingxi area, Ordos Basin. Nat Gas Indust B, 3(3): 216–225

Luo X, Wang Y, Li J, Liu H, Wang Y (2008). Origin of gas in deep Jiyang Depression. Nat Gas Indust, 29(9): 13−16+130−131 (in Chinese)

Meng Q, Sun Y, Tong J, Fu Q, Zhu J, Zhu D, Jin Z (2015). Distribution and geochemical characteristics of hydrogen in natural gas from the Jiyang Depression, Eastern China. Acta Petrol Sin (English ed), 89(5): 1616–1624

Ni Y, Dai J, Tao S, Wu X, Liao F, Wu W, Zhang D (2014). Helium signatures of gases from the Sichuan Basin, China. Org Geochem, 74: 33–43

Ni Y, Dai J, Zhu G, Zhang S, Zhang D, Su J, Tao X, Liao F, Wu W, Gong D, Liu Q (2013). Stable hydrogen and carbon isotopic ratios of coal-derived and oil-derived gases: a case study in the Tarim basin, NW China. Int J Coal Geol, 116−117: 302−313

Ping H, Chen H, Jia G (2017). Petroleum accumulation in the deeply buried reservoirs in the northern Dongying Depression, Bohai Bay Basin, China: new insights from fluid inclusions, natural gas geochemistry, and 1-D basin modeling. Mar Pet Geol, 80: 70–93

Prinzhofer A A, Huc A Y (1995). Genetic and post-genetic molecular and isotopic fractionations in natural gases. Chem Geol, 126(3-4): 281–290

Ren Y, Zhou Y, Cha M, Jin Q (2006). Maturity of Lower Tertiary source rocks in Dongying Depression. J China U Petrol, 30(2): 6−10 (in Chinese)

Shi B, Chang X, Xu Y, Wang Y, Mao L, Wang Y (2020a). Origin and migration pathway of biodegraded oils pooled in multiple-reservoirs of the Chepaizi Uplift, Junggar Basin, NW China: insights from geochemical characterization and chemometrics methods. Mar Pet Geol, 122: 104655

Shi B, Chang X, Xu Y, Mao L, Zhang J, Li Y (2020b). Charging history and fluid evolution for the Carboniferous volcanic reservoirs in the western Chepaizi Uplift of Junggar Basin as determined by fluid inclusions and basin modelling. Geol J, 55(4): 2591–2614

Shi B, Chang X, Yin W, Li Y, Mao L (2019). Quantitative evaluation model for tight sandstone reservoirs based on statistical methods−a case study of the Triassic Chang8 tight sandstones, Zhenjing area, Ordos Basin, China. J Petrol Sci Eng, 173: 601–616

Shen B, Huang Z, Liu H, Xu C, Yan Z, Chen M (2007). Geochemistry and origin of gas pools in the Gaoqing-Pingnan fault zone, Jiyang Depression. Chin J Geochem, 26(4): 446–454

Song M, Li Y (2020). Evaluation and practice of fine petroleum exploration in the Jiyang Depression. China Petrol Explor, 25(01): 93−101 (in Chinese)

Song M, Zhang X (2004). Discussion on deep gas geochemical characteristics and genesis of Bonan sag, Jiyang Depression. Nat Gas Geosci, 15(6): 646–649+675

Song Y, Yang L, Zhao J, Liu W, Yang M, Li Y, Liu Y, Li Q (2014). The status of natural gas hydrate research in China: a review. Renew Sustain Energy Rev, 31: 778–791

Su J, Zhu W, Lu H, Xu M, Yang W, Zhang Z (2009). Geometry styles and quantification of inversion structures in the Jiyang Depression, Bohai Bay Basin, eastern China. Mar Pet Geol, 26(1): 25–38

Tian J, Li J, Pan C, Tan Z, Zeng X, Guo Z, Wang B, Zhou F (2018). Geochemical characteristics and factors controlling natural gas accumulation in the northern margin of the Qaidam Basin. J Petrol Sci Eng, 160: 219–228

Vincent C J, Poulsen N E, Zeng R, Dai S, Li M, Ding G (2011). Evaluation of carbon dioxide storage potential for the Bohai Basin, northeast China. Int J Greenh Gas Control, 5(3): 598–603

Wang J, Li N (2020). Influencing factors and future trends of natural gas demand in the eastern, central and western areas of China based on the grey model. Natural Gas Industry B, 7(5): 473–483

Wang K, Pang X, Zhao Z, Wang S, Hu T, Zhang K, Zheng T (2017). Geochemical characteristics and origin of natural gas in southern Jingbian Gas Field, Ordos Basin, China. J Nat Gas Sci Eng, 46: 515–525

Wang L, Jin Q, Liu Y, Cheng F, Wang Z, Wu Y (2009). Genetic types of deep natural gas in Guxi Fault Zone in Jiyang Depression. Acta Sedment Sin, 27(01): 172–179

Wang L (2008). Genetic identification and generation and generation models of deep natural gas in Jiyang and Linqing Super-depression. Dissertation for the Doctoral Degree. Qingdao: China University of Petroleum(in Chinese)

Wang L, Jin Q, Lin L, Yin C, Song G (2007a). The geochemical

characteristics of natural gas and discussion on gas source in Bogu 4 buried hill. Nat Gas Geosci, 18(05): 715−719+749 (in Chinese)

Wang S, Vincent C J, Zeng R, Stephenson M H (2018). Geological suitability and capacity of CO_2 storage in the Jiyang Depression, east China. Greenhouse Gases: Sci Techn, 8(4): 747–761

Wang W, Li J, Tang H, Cui J, Kang Y (2007b). Genetic characteristics of associated gases from crudeoil biodegradation in Gudao Oilfield, Jiyang Depression. Oil Gas Geo, 28(3): 427−432 (in Chinese)

Wang Y, Kong X, Li Z (2010). Evolution of the Mesozoic source rocks in the Jiyang Depression. Nat Gas Indust, 30(4): 24−28+139 (in Chinese)

Wu X (2018). The tectonic characteristics of the strike slip field in the Jiyang Depression and its petroleum geological significance. Dissertation for the Doctoral Degree. Beijing: China University of Geosciences (in Chinese)

Wu X, Chen Y, Liu G, Zeng H, Wang Y, Hu Y, Liu W (2017). Geochemical characteristics and origin of natural gas reservoired in the 4th Member of the Middle Triassic Leikoupo Formation in the Western Sichuan Depression, Sichuan Basin, China. J Nat Gas Geosci, 2(2): 99–108

Wu X, Liu G, Liu Q, Liu J, Yuan X (2016). Geochemical characteristics and genetic types of natural gas in the Changxing-Feixianguan Formations from the Yuanba Gas Field in the Sichuan Basin, China. J Nat Gas Geosci, 1(4): 267–275

Yang X, Jiang Y, Geng C (2014). Origin and accumulation of cracking gas in the deep buried horizons in Jiyang Depression. Nat Gas Geosci, 25(8): 1226−1232 (in Chinese)

Yang T, Cao Y, Liu K, Wang Y, Zavala C, Friis H, Song M, Yuan G, Liang C, Xi K, Wang J (2019). Genesis and depositional model of subaqueous sediment gravity-flow deposits in a lacustrine rift basin as exemplified by the Eocene Shahejie Formation in the Jiyang Depression, eastern China. Mar Pet Geol, 102: 231–257

Zhang L (2012). Transfer structure and its petroleum significance of Jiyang Depression. Dissertation for the Doctoral Degree. Qingdao: China University of Petroleum (in Chinese)

Zhang L, Xu X, Liu Q, Kong X, Zhang S (2011). Hydrocarbon formation and accumulation of the deep Paleogene of the Jiyang Depression, Shengli Oilfield. Pet Explor Dev, 38(05): 530−537 (in Chinese)

Zhang X, Zhang T, Lin C, Wu X, Huang D, Lutome M S, Chen D, Liu W (2020). Reservoir architecture and evolution of meandering belt: a subsurface case in the Jiyang Depression, eastern China. J Petrol Sci Eng, 193: 107380

Zhang L (1991). Identifying criteria of natural gases in the Jiyang Depression. Petrol Geo Experi , 13(04): 355−369 (in Chinese)

Zhang S, Zhang L, Li Z (2009). Analysis of accumulation process of coal-formed gas in Gubei buried hill of Jiyang Depression. Nat Gas Geosci, 20(5): 670−677 (in Chinese)

Zhou J, Pang X, Li N (2006). Characteristics of hydrocarbon expulsion for the lower tertiary resource rocks in the Jiyang Depression, Bohai Bay Basin. Petrol Geo Experi, 28(01): 59−64 (in Chinese)

Zhu J, Hu Z, Lv J, Wang B, Zhou X (2010). Hydrocarbon generation history of upper Paleozoic source rocks of Jiyang and Linqing Depressions, Bohai bay basin. Petrol Geo Experi, 32(01): 58−63 (in Chinese)

Zhu G, Zhang S, Jin Q, Dai J, Zhang L, Li J (2005). Origin of the Neogene shallow gas accumulations in the Jiyang Superdepression, Bohai Bay Basin. Org Geochem, 36(12): 1650–1663

Zhu G, Jin Q, Zhang S, Zhang L, Li J (2006). Evolution of faulted lacustrine basin and hydrocarbon accumulation in Huimin Sag, Xinjiang. Petrol Geol, 27(01): 27−31 (in Chinese)